PROPORTIONAL-INTEGRAL-DERIVATIVE CONTROLLER IN

PROPORTIONAL NAVIGATION GUIDANCE

A Thesis

by

BYUNGJUN KIM

Submitted to the Office of Graduate and Professional Studies of
Texas A&M University
in partial fulfillment of the requirements for the degree of

MASTER OF SCIENCE

Chair of Committee,	Shankar P. Bhattacharyya
Committee Members,	Aniruddha Datta
	Garng M. Huang
	John E. Hurtado
Head of Department,	Miroslav M. Begovic

August 2016

Major Subject: Electrical Engineering

ABSTRACT

In this thesis, a Proportional-Integral-Derivative (PID) guidance scheme is discussed to improve the miss distance accuracy and the finite time stability problem in the Proportional Navigation Guidance (PNG). The primary goal of this study is to design the PID guidance that can accurately intercept the fast maneuvering target. The PID guidance is the extended version of the PNG with the integral and derivative terms in parallel. For the understanding of the conventional PNG model, the two-dimensional (2-D) engagement model of the missile and target is analyzed. Two characteristics are found in the PNG model: (1) its' stability is kept in the finite time but becomes unstable at the vicinity of the interception and (2) the Line-of-sight angle rate (LOSR) increases as the target acceleration magnitude increases.

To regulate the LOSR, the PID guidance is derived based on the servomechanism theory. The PID guidance model replaces the proportional gain of the conventional PNG model by the PID controller. A PID controller design using the numerical method through the iterative simulation is presented. For the various missile and target initial geometries, the capture region of the PID guidance is evaluated and compared with the conventional PNG model. In the end, the PID guidance model shows the improved miss distance accuracy, the extended stable time, and extended capture region when compared with the PNG model.

ACKNOWLEDGEMENTS

First of all, I would like to express my gratitude toward my advisor Prof. Shankar Bhattacharya for giving me a chance to study at Texas A&M University, motivating me to apply the servomechanism theory to the missile guidance problem. His guidance was precious to this study. I also would like to thank my committee members, Prof. Hurtado, Prof. Datta, and Prof. Huang for their guidance and support throughout the course of this work. Special thanks to Tammy Carda for her support to handle the difficulties other than class.

During this research, I got a great support from my fellow lab mates, Sangjin, Ivan, Narayani, Zhangxin, Randy, Miaomiao, Sunsoo, and Gi-hyeop. I would also like to express my gratitude to my research partner, Jaewon for his support.

Finally, thanks to my wife Sunyoung for her great sacrifice and love.

TABLE OF CONTENTS

LIST OF FIGURES

LIST OF TABLES

NOMENCLATURE

V = Velocity

V_c = Closing velocity

N' = Proportional Navigation Guidance gain

LOS = Line-of-sight

R = Missile-target range

λ = Line-of-sight angle

L = Lead angle

α = Missile flight path angle

β = Target flight path angle

y = Relative separation

t = Current time

t_f = Total flight time

τ = Missile time constant

Subscripts

M = Missile

T = Target

Superscript

$\cdot$ = Time differentiation

CHAPTER I

INTRODUCTION

The PNG is the most widely used guidance method in the surface-to-air missiles and its reliability has been proven for the past few decades. But with the performance evolution of the modern target, it is found that the missile system using the PNG might have a large miss distance for the modern airborne threats [1].

Thus, the missile guidance problem is approached using the servomechanism theory. The PID controller, one of the most famous classical controllers, is used to solve this problem; this shows the improvement in the system stability and miss distance accuracy.

For the first time, the conventional PNG system is studied through the 2-D nonlinear and linearized models. Next, the design parameter study of the PID guidance based on the servomechanism theory is investigated. Then, its performance is compared with the PNG. Finally, the designed PID guidance is validated in the three-dimensional (3-D) simulation model.

The designed PID guidance shows effectiveness by improving the miss distance and increasing the capture region.

I.1. General introduction of missile and guidance

A missile is defined as a flying weapon that has its own engine and can travel a long distance before exploding at the place at which it has been aimed [2]. Strictly,

missiles can be divided into two categories: (1) guided missiles or tactical missiles, and (2) unguided missiles or strategic missiles.

Typically, guided missiles include the following: (1) sensors (e.g., RF-seeker, Infrared-seeker), (2) a guidance system, (3) a warhead section, (4) a propulsion system, and (5) movable control surfaces. The guidance system places the missile on the proper trajectory to capture the target, and the control surfaces are deflected by commands from the guidance system in order to direct the missile in flight [3].

Additionally, missiles can be classified on the basis of their launch mode: (1) Surface-to-Surface missile, (2) Surface-to-Air missile, (3) Air-to-Air missile, and (4) Air-to-Surface missile.

The type of missile handled in this study is the Surface-to-Air guided missile. One example is the US Navy's Standard Missile 2 (SM-2). The SM-2 is the primary Surface-to-Air air defense missile of 15 countries including the US, South Korea, Japan, and Australia. It uses the tail controls and a solid fuel rocket motor for propulsion and maneuverability [4]. General specifications of SM-2 are listed in Table 1.

Table 1. General specifications of Standard Missile 2

Range	90 nautical miles
Length	15 feet, 6 inches (4.72m)
Diameter	13.5 inches (34.3cm)
Weight	1,558 pounds (708kg)
Wingspan	3 feet 6 inches (1.08m)
Guidance system	Semi-active radar
Warhead	Radar and contact fuse, blast-fragment warhead
Propulsion	Dual thrust, solid rocket fuel

Missile guidance is defined as the strategy for steering the missile to achieve the interception with the target [5]. In order for the missile to intercept a maneuverable target with little miss distance, guidance uses the principles of feedback control [6]. The guidance generates acceleration command to shape the collision course between the missile and the evasive target.

Missile guidance is generally divided into three phases - boost, midcourse, and terminal. Figure 1 shows the general phases of missile guidance. Terminal phase is the last stage of the missile guidance and it requires a high accuracy and fast response. The PNG is the most widely used terminal guidance technique for homing missiles because of its simplicity and reliability, since it was first discovered by Germans during World War II [3].
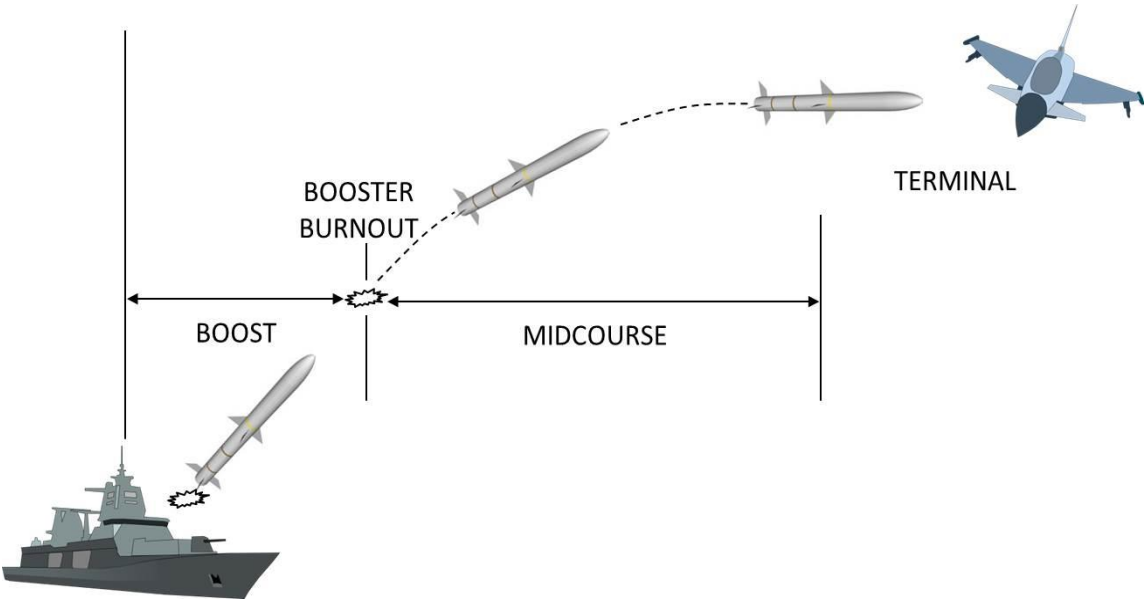
Figure 1. General phase of missile guidance

I.2. Proportional Navigation Guidance

Many of the modern guided missiles use the PNG or its variants for their terminal guidance because of its simplicity and reliability. Historically, the PNG was first discovered by the Germans during World War II at Peenemünde Research Center, but it was first successfully applied to the U.S. "Lark" .

The PNG uses the condition of collision triangle to intercept the target. According to the condition of collision triangle, the collision will happen if the angle of direction of the other entity is kept unchanged and the relative range between them decreases.

The PNG is based on the derived first condition of the collision triangle: the rate of change of the angle direction with other entity is zero. To satisfy the first condition of the collision triangle, the PNG rotates the missile that is proportional to the rate of change of the angle of direction. Hence, if the PNG works perfectly, the collision condition is satisfied and the interception is guaranteed.

The PNG generates the lateral acceleration command to steer the missile heading. The generated acceleration command is employed by the flight control system that makes relevant aerodynamics using a control fin to achieve the commanded acceleration. Detailed characteristics of the PNG are studied in Chapter II.

I.3. Feedback control and servomechanism theory

In engineering systems, there are many cases of the requirement of having the system's output track a reference signal. The feedback control provides this ability. The

feedback control makes corrective action using the error between the reference and output in order to bring the actual output closer to the reference. Missile guidance system is based on the feedback control.

Servomechanism theory is a reference tracking ability despite the inherent uncertainties and changes in the plant dynamics [7]. The core of the servomechanism theory is based on an integrator. In brief, if the plant is stable and the output of the integrator is constant for a finite time, the input of the integrator must be zero at the same time. In this study, the strength of the integrator is used to improve the missile performance. The theory of servomechanisms will be studied in chapter III with details.

PID type is the most widely used controller in the servomechanism problems. The PID controller is based on an integrator and it has three adjustable parameters k_p, k_i, and k_d. With this 3 degrees-of-freedom, the PID controller has sufficient ability for attaining stability and a fast transient response. From this structure, the PID controller can yield excellent results in many applications.

I.4. Issues in Proportional Navigation Guidance

Because of its simple structure and ease of implementation, the PNG had been widely used through the 1960s and early 1970s. PNG requires low levels of information regarding the target motion, such as line-of-sight angle rate (LOSR) and closing velocity. These low information requirements simplify the onboard sensor and improve reliability and robustness of the missile system [8].

But by the mid-1970s, the evolved airborne threats such as modern jetfighters and supersonic missiles made the interceptor missiles based on the PNG face its performance limit. In other words, the collision triangle is broken since the interceptor missile cannot maintain the LOSR to zero.

One solution to this problem is to apply an optimal control theory to the missile guidance.

I.4.1. Optimal guidance

With the advent of modern airborne threats in the mid-1970s, higher missile performance was required. By that time, the optimal control theory had sufficiently matured, and the modern computer progressed to compute the advanced algorithms. So, the optimal guidance became the alternative guidance law design [1]. The strength of the optimal guidance is a missile can be sure to intercept the target with the minimum acceleration requirement. But the complexity of the system followed. Another approach of modern guidance is through the theory of servomechanisms.

I.4.2. Guidance using servomechanism theory

The strength of an integrator can be applied to solve the problem of PNG. Essentially, from the perspective of a control system, the PNG is a regulator problem that drives the LOSR to zero. Using the servomechanism theory, by taking the LOSR as the input of the integral, it is possible to bring the LOSR to zero. Then, a guidance system without a miss distance can be made. Standard controllers, such as Proportional

Integral (PI) and PID, can be used in the above regulator problem. The simplicity of the system is the strength of this approach.

I.5. Literature review

The literature on using the servomechanism theory for the missile guidance problem is reviewed. Gonsalves et al show the fuzzy logic based PID guidance has higher accuracy and faster response time [9]. Lin et al show the PID guidance has a wider bandwidth than the PNG and Augmented Proportional Navigation(APN) [10]. Rogers tested PID, PI, and lead controller in the guidance problem and shows that the missile performance is improved when the controller parameter degrees of freedom is increased [11]. Golestani et al show the PID guidance has a larger stability region compared with the PNG, Proportional Derivative (PD) guidance and PI guidance [12]. These researchers demonstrate the classical PID controller could improve the missile guidance performance. All of them give precious knowledge to this field. However, the capture region of the PID guidance is not studied yet considering the uncertainty of initial relative position of the missile and target.

I.6. Research objective

As discussed in the previous section, the various methods for designing the missile guidance using servomechanism theory has been studied in the literature. Although a number of different approaches exist which address these problems separately, none of the discussed methods covered how much the PID guidance can

improve the capture region. The goal of this research is (a) to design a PID guidance in 2-D model which minimizes the miss distance and increases the capture region, (b) and to expand to a 3-D simulation model.

I.7. Research brief

This paper is organized as follows: chapter II builds an analysis of PNG with 2-D nonlinear and linearized model. Then, the concept of servomechanism theory and PID guidance are introduced in chapter III. Design process of PID guidance and the performance comparison between the PID guidance and the PNG are handled in chapter IV. Furthermore, the designed PID guidance is validated its effectiveness in a 3-D simulation model in chapter V. The results of this study are summarized in chapter VI.

CHAPTER II

PROPORTIONAL NAVIGATION GUIDANCE

Since the PNG is based on the 1st condition of the collision triangle, the concept of the collision triangle should be understood beforehand. Next, from the differential equations of 2-D missile and target engagement geometry, the nonlinear model and linearized model are built and analyzed. The mathematical model and linearization procedure are taken from Zarchan [13] and the Matlab/Simulink models are taken from Bucco et al [14].

II.1. Collision triangle and collision condition

The goal of the missile guidance system is to steer a missile heading to collide with a target. The collision theory goes back to the old sailor's saying, which predicts the collision with other ships. This is called, 'Constant Bearing, Decreasing Range' (CBDR).

To predict the potential of collision at sea, many academic works for how to find what conditions make the collision and how to prevent it have been done [15, 16]. Inversely, this collision condition was applied to a missile guidance technique to intercept a target.
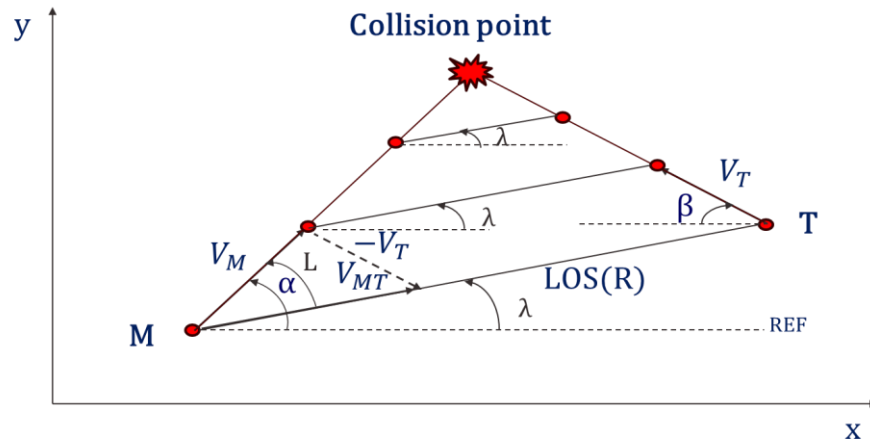
Figure 2. Geometry of collision triangle

Figure 2 shows the geometry of the collision triangle. The collision triangle is defined as the triangle formed by the initial positions of missile and target, and the intercept point where the missile hits the target when flown in a straight line [17]. Both missile and target are assumed to maintain consistent speed and velocity. To predict the collision, the relative velocity plays an important role. The relative velocity is defined as the vector difference between the velocities of two bodies: the velocity of a body with respect to another regarded as being at rest [18]. For example, the target is set as a reference and the relative velocity is calculated. The relative velocity vector is obtained by subtracting the target's velocity V_T from the missile's velocity V_M. The new vector V_{MT} becomes the missile's velocity relative to the target while the target is regarded as standing still. If the relative velocity vector points towards on target, the collision will happen. Furthermore, since the missile and the target velocities are constant, the relative velocity is also constant. So, the target senses the missile is

approaching from the constant direction. Inversely, the missile looks at the target in the direction of the other side constantly.

Hence, the first condition of the collision triangle is the LOS angle λ is constant. This is same as the rate of change of the LOSR is zero. The second condition of the collision triangle is the LOS distance R should decrease. These two conditions can be expressed mathematically,

$$\lambda = constant \quad or \quad \dot{\lambda} = 0 \tag{1}$$

$$\dot{R} < 0. \tag{2}$$

The PNG is based on the 1st condition of the collision triangle. But of course, a target can notice an interceptor missile and it counter with an evasive maneuver. Hence, the mission of the PNG is meeting and keeping the collision condition against a maneuvering target.

II.2. Two-dimensional nonlinear model

II.2.1. Mathematical model

The role of the PNG is satisfying the 1st condition of the collision triangle, which is bringing the LOSR to zero. Essentially, the PNG rotates the missile heading at a rate that is proportional to the LOSR. If the PNG works perfectly, the LOSR should converge and stay at zero until interception.

The output of the PNG is the lateral acceleration command. Mathematical form of the PNG is:

$$n_c = N'V_c\dot{\lambda} \tag{3}$$

where n_c is the acceleration command (m/s^2), N' is the design variable known as the effective navigation ratio, V_c is the closing velocity (m/s), and $\dot{\lambda}$ is the LOSR. N' is practically chosen between 3 and 5 because of the system noise effect [13].

To build an engagement model based on the PNG, consider a 2-D missile-target engagement under some assumptions. The missile and the target velocities are both constant and gravity force is negligible. The geometry of the engagement is shown in Figure 3,
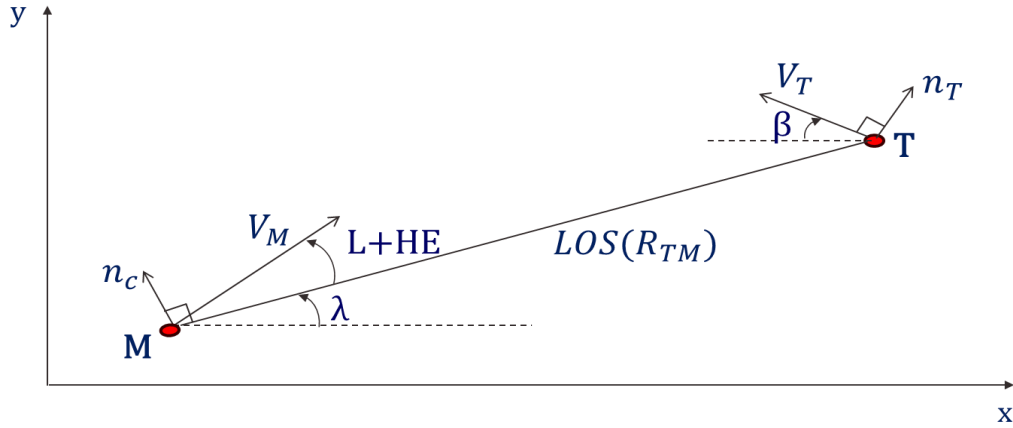
Figure 3. 2-D Missile and target engagement geometry

where the capital M and T denote the missile and the target, respectively. V_M and V_T mean the missile and target velocities, respectively. The straight line between the missile and the target is LOS and the range of the LOS is denoted as R. The angle between the LOS and the x-axis is λ. α and β are the missile and the target velocity angles. n_c is the missile acceleration command, which is generated by PNG, and n_T is the target acceleration. The angle L is called the missile lead angle. Theoretically, the lead angle is

12

the correction angle for the missile to make the collision course with the target. As soon as L is calculated, the missile will intercept the target unless the target does not change its heading or speed. The mathematical form of the lead angle can be derived by using the law of sine:

$$L = \sin^{-1}\left(\frac{V_T \cdot \sin(\beta + \lambda)}{V_M}\right) \tag{4}$$

The nonlinear differential equations for the target motion are,

$$\dot{R}_{TX} = -V_T \cos(\beta) \tag{5}$$

$$\dot{R}_{TY} = V_T \sin(\beta) \tag{6}$$

$$\dot{\beta} = \frac{n_T}{V_T} \tag{7}$$

where R_{TX} and R_{TY} are the X and Y components of the target position and the dot over the variables presents the differentiation with respect to time. The negative sign in the term $\dot{R}_{TX}$ comes from the projection of $\dot{R}_T$ onto the x-axis. Note that the subscripts T and M indicate target and missile where X and Y indicate the related axes.

Similarly, the nonlinear equations for the missile motion are,

$$\dot{R}_{MX} = V_{MX} \tag{8}$$

$$\dot{R}_{MY} = V_{MY} \tag{9}$$

$$\dot{V}_{MX} = -n_c \sin(\lambda) \tag{10}$$

$$\dot{V}_{MY} = n_c \cos(\lambda) \tag{11}$$

where, R_{MX}, R_{MY} are the X and Y components of the missile position and V_{MX}, V_{MY} are the X and Y components of the missile velocity.

Relative motion equations between the missile and the target can be derived,

$$R_{TMX} = R_{TX} - R_{MX} \tag{12}$$

$$R_{TMY} = R_{TY} - R_{MY} \qquad (13)$$

where (R_{TMX}, R_{TMY}) defines X, Y components of the relative separation of the missile and the target. And the range between the missile and the target can be obtained by application of the distance formula,

$$R_{TM} = \sqrt{R_{TMX}^2 + R_{TMY}^2} \qquad (14)$$

The closing velocity can be defined as a negative rate of change of the range between the missile and the target. Therefore,

$$V_C = -\dot{R}_{TM} = \frac{-(R_{TMX}V_{TMX} + R_{TMY}V_{TMY})}{R_{TM}} \qquad (15)$$

While the LOS angle λ can be derived by considering the projection of the range R_{TM} on the X and the Y axes,

$$\lambda = \tan^{-1}\left(\frac{R_{TMY}}{R_{TMX}}\right) \qquad (16)$$

The LOSR can be derived from the first derivative of the LOS angle λ:

$$\dot{\lambda} = \frac{R_{TMX}V_{TMY} - V_{TMX}R_{TMY}}{R_{TM}^2} \qquad (17)$$

When the variables in Eq.3 are replaced with the ones in Eq.15 and Eq.17, the magnitude of the missile acceleration command can be defined as:

$$n_c = N' \cdot \frac{-(R_{TMX}V_{TMX} + R_{TMY}V_{TMY})}{R_{TM}} \cdot \frac{R_{TMX}V_{TMY} - V_{TMX}R_{TMY}}{R_{TM}^2} \qquad (18)$$

where N' is a chosen constant.

To complete the engagement model, some additional initial conditions and assumptions are required. In reality, the missile is not launched exactly on a collision course. The expected intercept point cannot be calculated precisely because it is unable to predict the target's future action. So, the initially predicted intercept point is only

approximated with limited information. Naturally, there is some deviation between the actually launched direction and the ideal collision course. Any initial angular deviation of the missile from the collision course is known as a heading error *HE*. Accordingly, the initial missile velocity components can be expressed with the lead angle *L* and the actual heading error *HE* as

$$V_{MX}(0) = V_M \cos(L_0 + HE_0 + \lambda_0) \quad\quad (19)$$

$$V_{MY}(0) = V_M \sin(L_0 + HE_0 + \lambda_0) \quad\quad (20)$$

The zero terms in the equations mean the initial conditions. And if we model the actual acceleration of the missile n_M by a first order lag term, then

$$\frac{n_M}{n_C} = \frac{1}{1+\tau s} \quad\quad (21)$$

Using the differential equations listed above a 2-D nonlinear missile and target engagement model is made with MATLAB/Simulink. The top level Simulink model is showed in Figure 4[14]. Initial condition and specification of the missile and the target are given in Table 2.
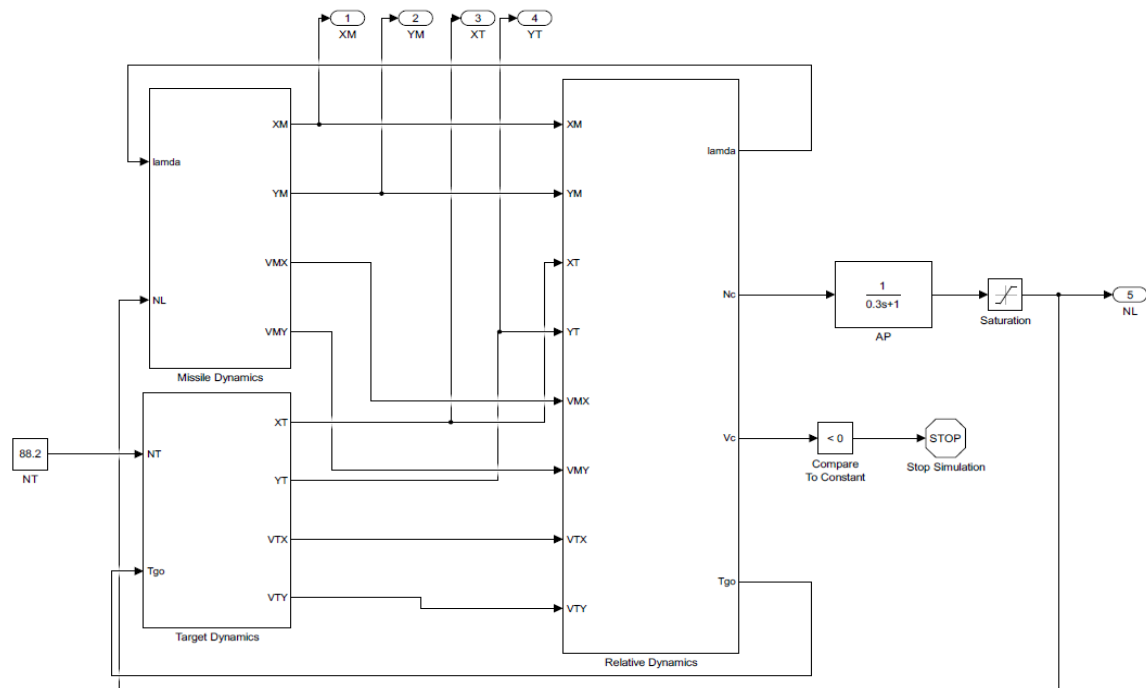
Figure 4. 2-D nonlinear engagement model in Simulink
© *Commonwealth of Australia 2013*

Table 2. Initial condition of 2-D Non-maneuvering target simulation

Missile		Target	
X-axis position(m)	0	X-axis position(m)	11,000
Y-axis position(m)	0	Y-axis position(m)	3,000
Velocity(m/s)	700	Velocity(m/s)	500
Flight velocity angle(°)	0	Flight velocity angle(°)	0
Effective navigation ratio N′	3	Acceleration(G force)	0
Time constant(s)	0.1		
Maximum acceleration(G force)	20		

16

II.2.2. Simulation results

Using the above Simulink model, the performance of the PNG is studied under the three types of target maneuvering scenarios. The simulated scenarios are,

(i)   Non-maneuvering target

(ii)   Slow maneuvering target

(iii)   Fast maneuvering target

The simulation result of the PNG model will be compared with the PID guidance model in chapter III.

II.2.2.1. Non-maneuvering target

Consider a case when the target aircraft does not notice the existence of the defense missile, so it maintains its initial heading and speed. This case can be unrealistic because the fighter aircraft has a radar warning receiver to detect the threat's radar signal. The purpose of this simulation is to study how the PNG works against the simplest target.

According to the initial conditions in Table 2, the altitudes of the missile and the target are different. The initial flight path angles of missile and target are zero, so the missile is not on a collision course with the target at the start point of the terminal guidance. Nevertheless, the missile can hit the target easily since the PNG corrects the missile flight course to the collision course. The trajectory of the missile and the target is shown in Figure 5.A. Once the missile flight course is corrected, the missile flies in a straight line to the predicted intercept point because the target flight course is constant.

Figure 5.B shows the missile acceleration generated by the PNG during the flight time. The magnitude of missile acceleration is very small since the PNG only has to generate the acceleration command which makes the lead angle. We can see that the non-maneuvering target is the very easy case for the PNG.
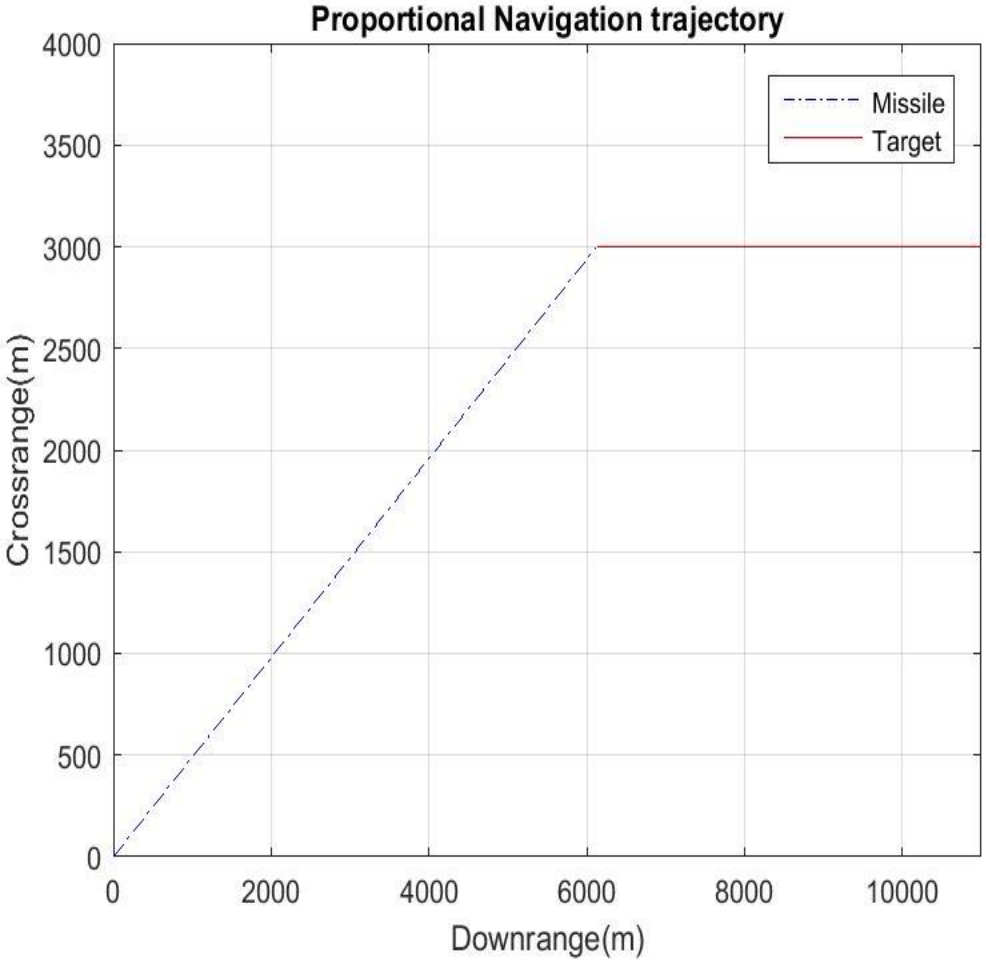
Figure 5.A. PNG trajectory with non-maneuvering target ($n_T = 0$)
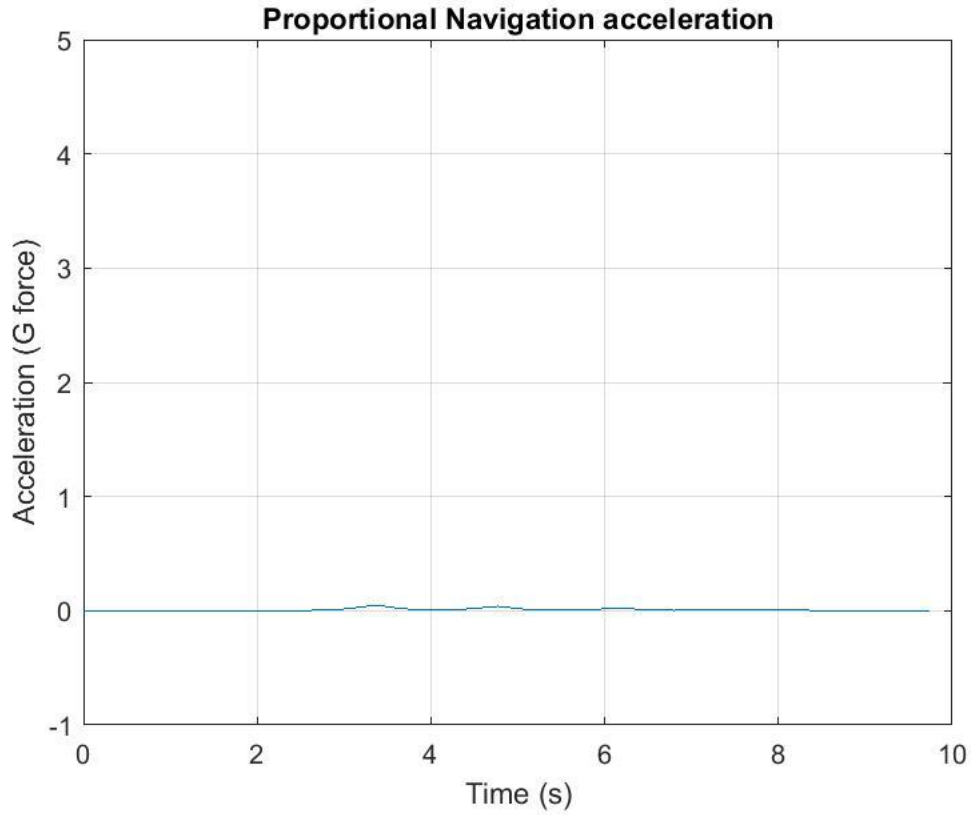
Figure 5.B. PNG acceleration with non-maneuvering target ($n_T = 0$)

II.2.2.2. Slow maneuvering target

Let us consider a more practical case. The target notices the existence of the defense missile so it maneuvers with a constant acceleration, 3G from the start point of the terminal phase. The missile and the target are at the same altitude and the other initial conditions are given in Table 3.

Figure 6.A shows a trajectory of the missile with the maneuvering target when the effective navigation ratio N' is 3. The target initially changes its course upwards and

19

makes a steadily rising curve. In the same manner, the missile makes a steadily rising curve and accurately hit the target at the end of the flight.

Figure 6.B shows the missile acceleration graph against the slow maneuvering target. The acceleration increases monotonically for most of the flight time. Note that the highest acceleration generated by the PNG is quite higher than the target acceleration (3G) [13].

Figure 6.C shows the LOSR graph. The small amount of LOSR linearly increases until right before the interception then it goes to infinity. The reason of this instability at interception time comes from the LOSR equation (17). Since the denominator R_{TM} decreases during the flight time and it goes to zero at the end of the interception, the LOSR goes to infinity. But note that the PNG system keeps the LOSR small to the slow maneuvering target during the most of the flight time and, this is closely related to the miss distance accuracy. The miss distance and the intercept time are shown in Table 4.

Table 3. Initial condition of 2-D Maneuvering target simulation

Missile		Target	
X-axis position(m)	0	X-axis position(m)	11,000
Y-axis position(m)	3,000	Y-axis position(m)	3,000
Velocity(m/s)	700	Velocity(m/s)	500
Flight velocity angle α(°)	0	Flight velocity angle β(°)	0
Effective navigation ratio N′	3 ~ 5	Acceleration(G force)	0 ~ 10
Time constant(s)	0.1		
Maximum acceleration(G force)	20		

Figure 6.A. PNG trajectory in case of 3G step in target maneuver ($N^{'} = 3$)

Figure 6.B. PNG acceleration in case of 3G step in target maneuver ($N' = 3$)
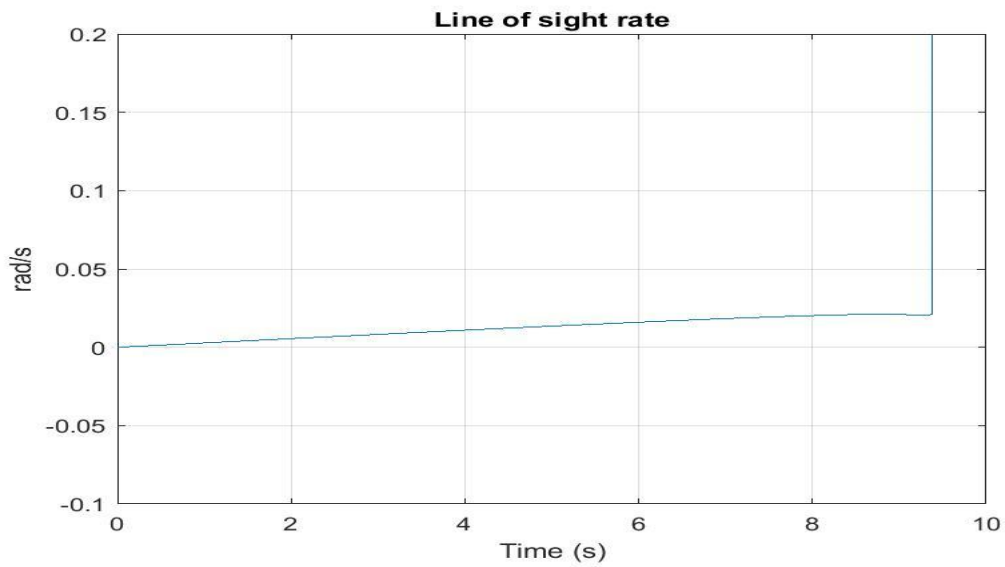
Figure 6.C. PNG LOSR in case of 3G step in target maneuver ($N' = 3$)

Table 4. 2-D nonlinear model results (n_T=3G)

Intercept time(s)	Miss distance(m)
9.400	0.000

This simulation shows that the PNG is effective against the slow maneuvering target. The LOSR is small and bounded until right before the interception. In other words, the 1st condition of the collision triangle is satisfied for the most of the flight time.

II.2.2.3. Fast maneuvering target

Practically, the modern jetfighter has a fast maneuvering capability. It makes the most of its ability to evade the defense missile. So the missile should have the capability

to track the fast maneuvering target. Furthermore, the actual maximum acceleration of the missile is limited. Hence, the guidance command should not exceed the acceleration limit. The performance of the PNG is tested with the maximum acceleration of the target (10G) shown in Table 3.

The missile and target trajectory is shown in Figure 7.A. At the early stage, the missile rotates upward to track the rising target. After passing the middle point, the missile rotates to a downward direction to follow the rotating target. But at the end of flight, the missile misses the target by a large distance because it cannot rotate fast to chase the agile target.

Figure 7.C shows that the LOSR diverges from the middle point. It is clear that the PNG with the effective navigation ratio(N') 3 is ineffective to the fast maneuvering target.
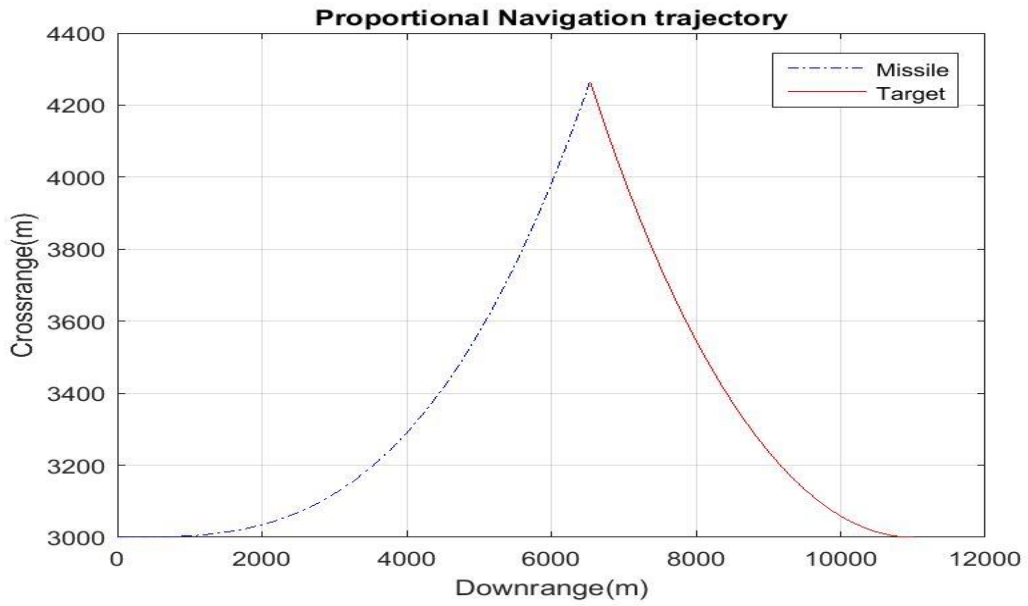

Figure 7.A. PNG trajectory in case of 10G step in target maneuver ($N' = 3$)

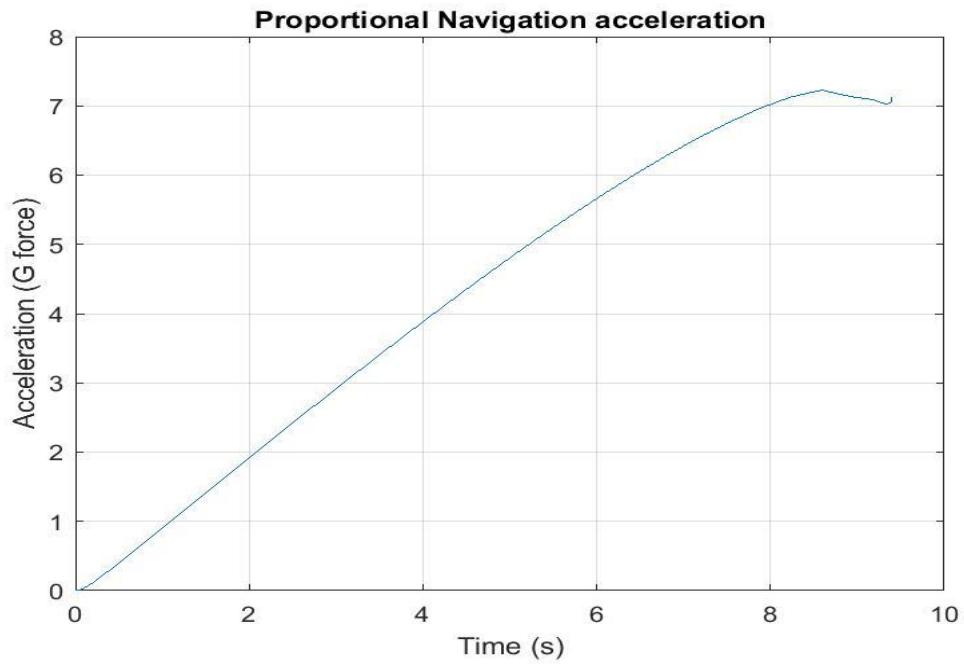Figure 7.B. PNG acceleration in case of 10G step in target maneuver ($N' = 3$)

Figure 7.C. PNG LOSR in case of 10G step in target maneuver ($N' = 3$)

To check the effect of the control variable, the effective navigation ratio(N') is changed between 3 and 5 with the fast maneuvering target. The missile and target trajectories are shown in Figure 8.A. We can see that higher gain causes the missile to rotate slightly faster than the lower gain. Figure 8.B shows that the higher gain generates faster missile acceleration than the lower gain. From the Figure 8.C, we can see that the higher gain causes the small LOSR and extends the stable time. This small LOSR error and extended stability implies the better accuracy of Table 5. But the miss distance 26.243m, when the gain is 5, is not a satisfactory performance for the precision missiles.
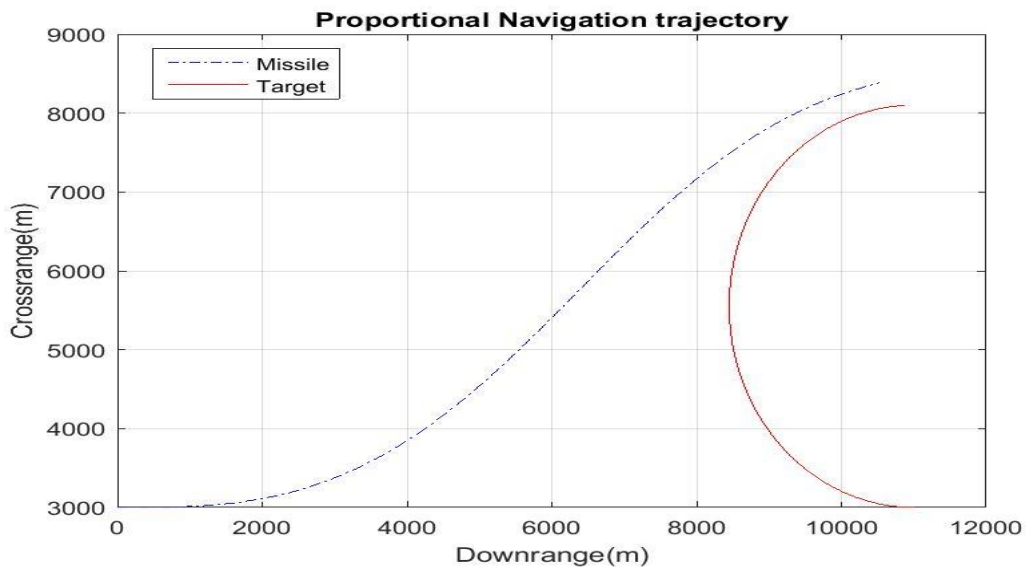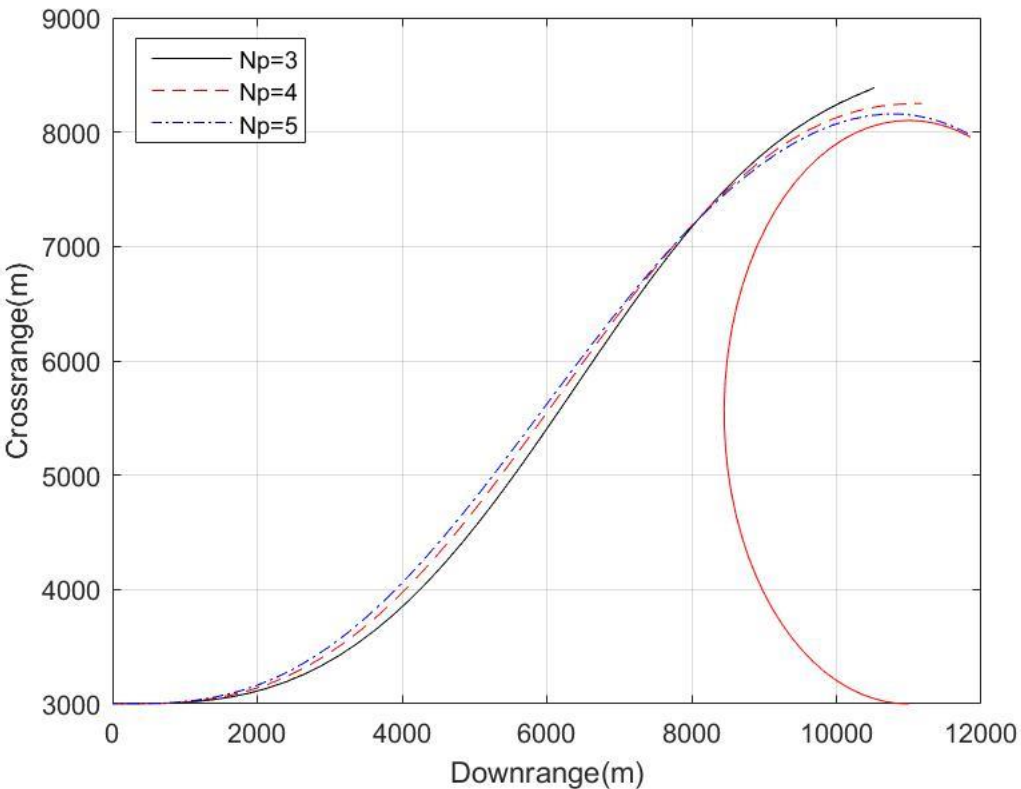

Figure 8.A. PNG trajectory in case of 10G step in target maneuver (N'=3~5)

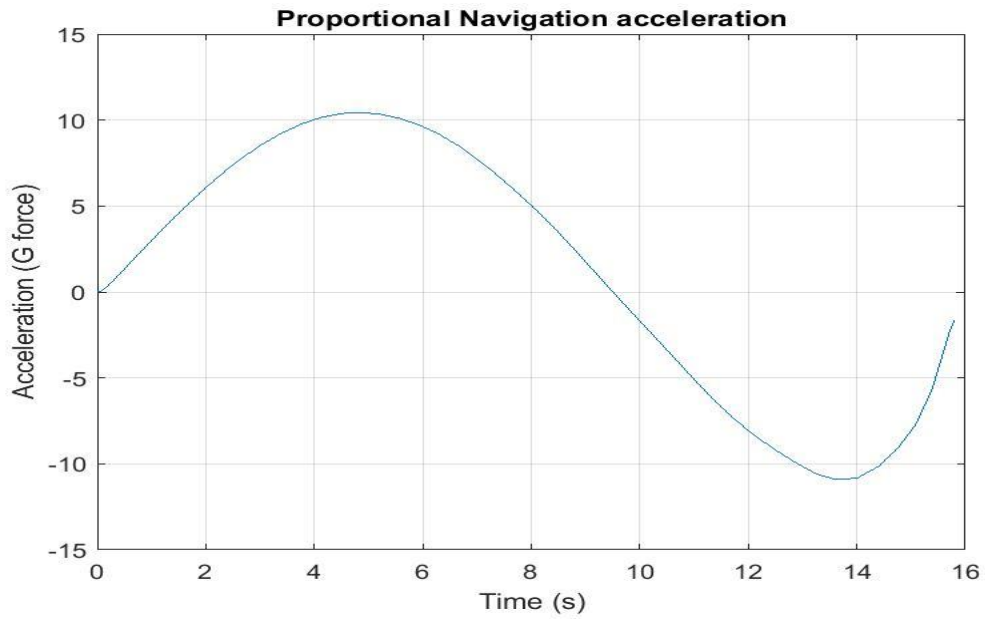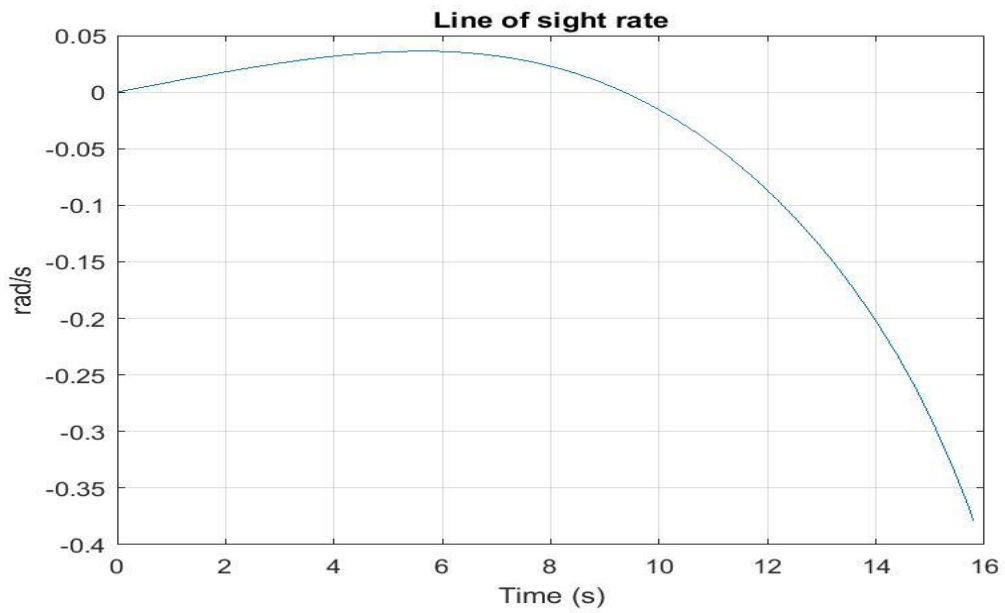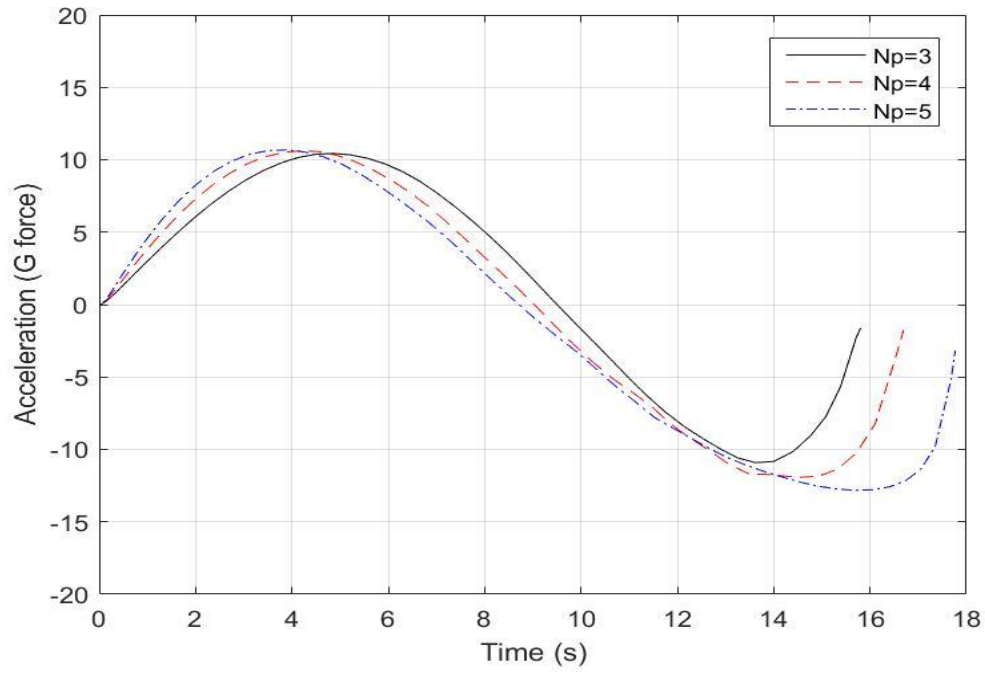Figure 8.B. PNG acceleration in case of 10G step in target maneuver (N'=3~5)
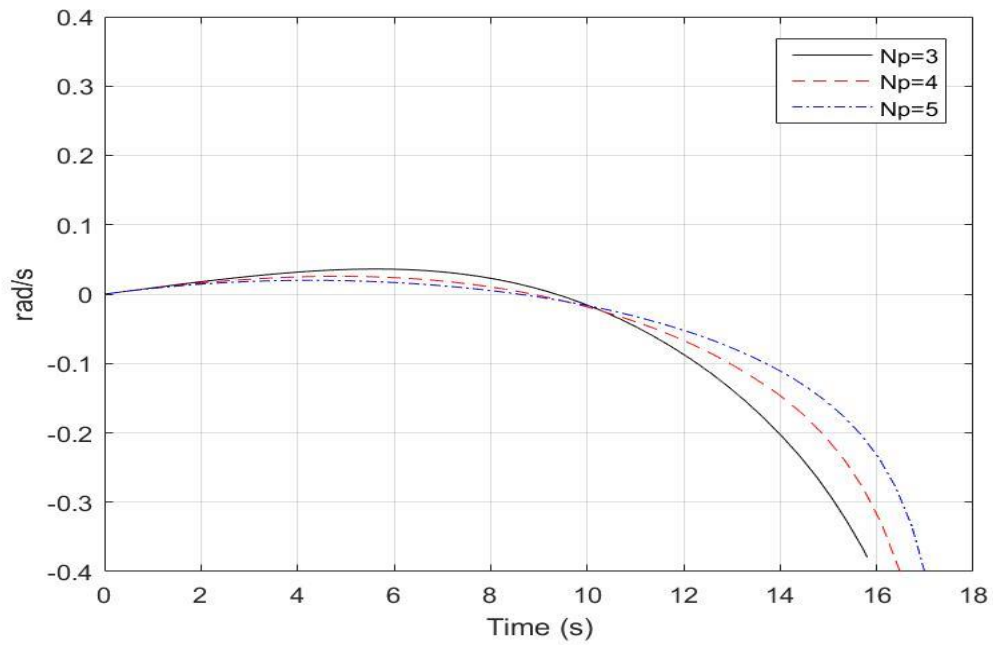
Figure 8.C. PNG LOSR in case of 10G step in target maneuver (N'=3~5)

26

Table 5. Miss distance results when $N' = 3 \sim 5$

N'	Intercept time(s)	Miss distance(m)
3	15.803	462.794
4	16.693	227.898
5	17.768	26.243

From this simulation, we can see that the conventional PNG is effective to the slow maneuvering target. But the PNG shows its limit of performance to fast maneuvering target under the limited range of the proportional gain.

The 2-D nonlinear simulation shows the system characteristics and the performance limit of the PNG model. But the reason why the PNG performance is degraded against the fast maneuvering target is not clearly shown in the nonlinear model. To get a deeper understanding of the conventional PNG model, the linearized model is derived.

II.3. Two-dimensional linearized model

The linearization technique is employed for the analysis of the PNG model. Generally, a linearized model is a simple approximation of a nonlinear model that is only valid in a small region around an operating point. But we can apply linear control theories to get valuable understanding about the relationship between the variables. This understanding becomes a hint to design a controller to solve the conventional system's problem.

II.3.1. Mathematical model

Linearization of the previous 2-D nonlinear engagement model is developed with the simplest situation: the missile and the target flight path angles are small (near head-on or tail chase case). Figure 9 shows the 2-D missile and target engagement model for the linearization.
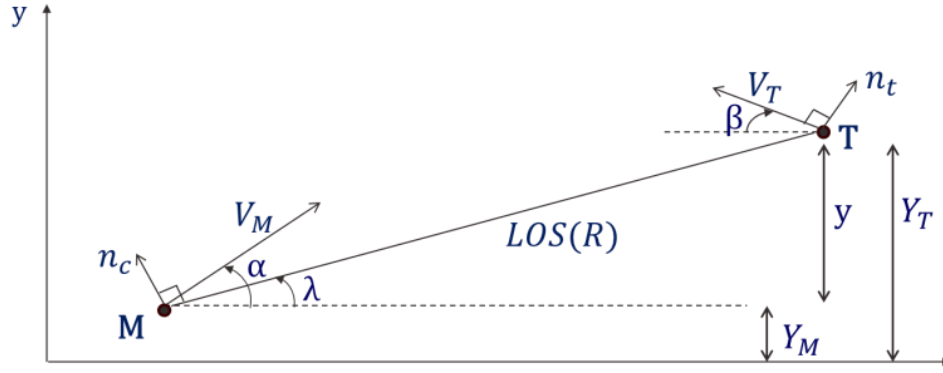
Figure 9. 2-D Engagement model for linearization

The first step of linearization is defining the new relative state. The relative separation between the target and the missile orthogonal to the fixed reference is defined in Figure 9:

$$y = Y_T - Y_M \qquad (22)$$

The relative acceleration (difference between target and missile acceleration) is expressed using the trigonometrical function:

$$\ddot{y} = n_{TY} - n_{MY} = n_T \cos(\beta) - n_c \cos(\lambda) \qquad (23)$$

For small angles, the cosine terms are approximated to unity, and the previous Eq. 23 is linearized to,

$$\ddot{y} = n_T - n_c \qquad (24)$$

28

Likewise, the sine terms are approximated to an angle itself, so the LOS angle λ is linearized to,

$$\sin \lambda = \lambda = \frac{y}{R} \qquad (25)$$

The closing velocity between missile and target is approximated for the two cases. At first, the head-on case is

$$V_c = V_M + V_T \qquad (26)$$

While the tail chase case is

$$V_c = V_M - V_T \qquad (27)$$

The range of the missile and target is approximated with multiplication of the closing velocity and the time until intercept:

$$R = V_c(t_F - t) \qquad (28)$$

where t denotes the current time and t_F the total flight time of the engagement.

In the 2-D engagement scenario, the objective of the missile guidance is minimizing the relative separation y at the end of the flight. Hence, the linearized miss distance (MD) can be defined as:

$$MD = y(t_F) \qquad (29)$$

Since the linearized miss distance is not calculated from the distance formula, it is only an approximation of the nonlinear model miss distance.

Using the listed equations, the linearized PNG homing loop is constructed, show in Figure.10. We can see that the PNG system is based on a feedback control.
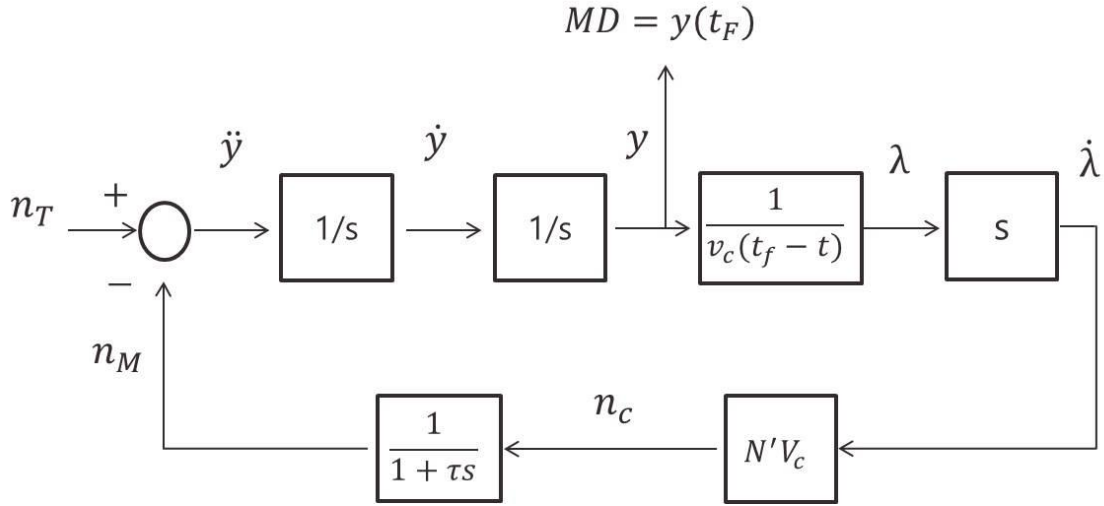
Figure 10. Linearized PNG homing loop model

The block *s* in the block diagram refers to a differentiator in the frequency

domain. Since the above diagram includes the pure differentiator, it is impossible to

make a state space model directly. To solve this problem, the block diagram

manipulation is used to construct the equivalent model. This can be derived using

differentiation of the linearized LOS angle equation in equation (25). The linearized

LOS angle can be expressed again using the above range equation (28):

$$\lambda = \frac{y}{R} = \frac{y}{V_c(t_F - t)} \tag{30}$$

After differentiating the above equation, the rate of change of the LOS angle (LOSR) is

derived as:

$$\dot{\lambda} = \frac{y + \dot{y}(t_F - t)}{V_c(t_F - t)^2} \tag{31}$$

Replacing this new LOSR term at the previous linearized model Figure 10, the alternative block diagram of the linearized PNG homing loop is achieved in Figure 11 [14].

$$MD = y(t_F)$$
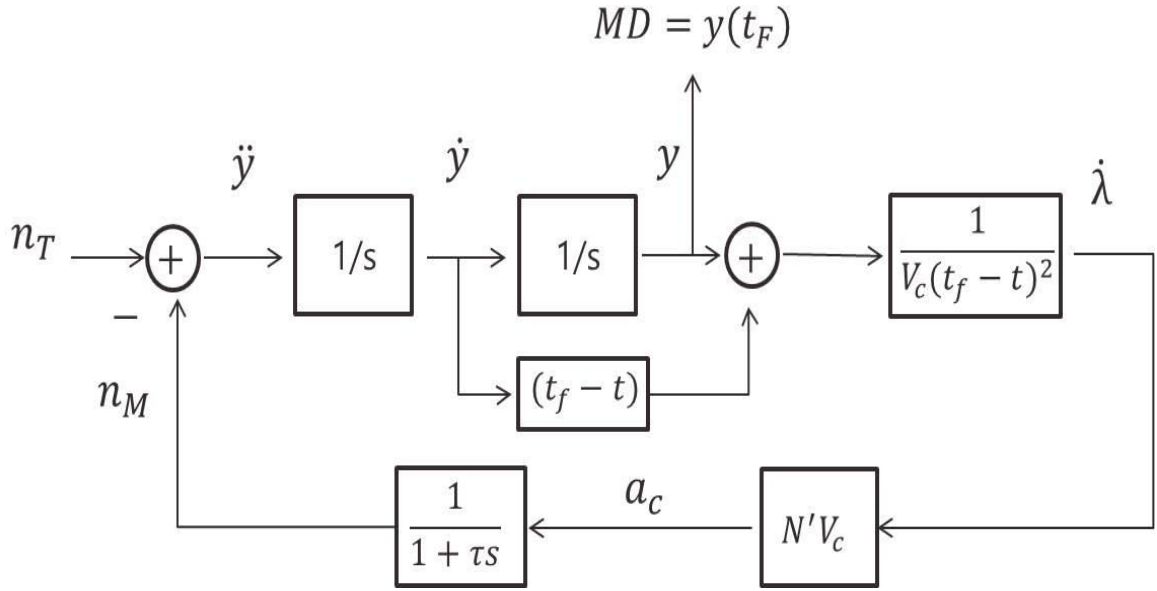
Figure 11. Alternative linearized PNG homing loop model

The linearized PNG missile acceleration command n_c can be derived by substituting the LOSR term in the equation (3) with the equation (31).

$$n_c = N' \, V_c \, \dot{\lambda} = \ N' \, V_c \, \frac{y + \dot{y}(t_f - t)}{V_c(t_f - t)^2} = \ N' \frac{y + \dot{y}(t_f - t)}{(t_f - t)^2} \qquad (\,32\,)$$

The alternative linearized PNG model is used for the analysis of the original model. For the state-space representation of the alternative linearized PNG model, let us choose the state variables as relative separation (y), relative velocity ($\dot{y}$), and actual acceleration of missile (n_M). The input of the system is target acceleration (n_T) and the outputs are the relative separation (y) and the actual acceleration of missile (n_M).

$$x_1 = y \qquad (\,33\,)$$

31

$$x_2 = \dot{y} \tag{34}$$

$$x_3 = n_M \tag{35}$$

$$u = n_T \tag{36}$$

$$y_1 = y \tag{37}$$

$$y_2 = n_M \tag{38}$$

From the 1$^{\text{st}}$ order missile dynamics model in equation (21), the differential equation of the actual acceleration can be derived using the inverse Laplace transformation,

$$\dot{n}_M = \frac{1}{\tau}(n_c - n_M) \tag{39}$$

Then the states equations are

$$\dot{x}_1 = x_2 \tag{40}$$

$$\dot{x}_2 = n_T - n_M = u - x_3 \tag{41}$$

$$\dot{x}_3 = \frac{1}{\tau}(n_c - n_M) = \frac{1}{\tau}\left(N'\frac{y + \dot{y}(t_f - t)}{(t_f - t)^2} - n_M\right) = \frac{N'x_1}{\tau(t_f - t)^2} + \frac{N'x_2}{\tau(t_f - t)} - \frac{x_3}{\tau} \tag{42}$$

$$y_1 = x_1 \tag{43}$$

$$y_3 = x_3 \tag{44}$$

From the above differential equations, the state-space representation is

$$\dot{x} = \begin{bmatrix} 0 & 1 & 0 \\ 0 & 0 & -1 \\ \frac{N'}{\tau(t_f - t)^2} & \frac{N'}{\tau(t_f - t)} & -\frac{1}{\tau} \end{bmatrix} x + \begin{bmatrix} 0 \\ 1 \\ 0 \end{bmatrix} u \tag{45}$$

$$y = \begin{bmatrix} 1 & 0 & 1 \end{bmatrix} x \tag{46}$$

From the state-space model, it is observed that the 3$^{\text{rd}}$ state n_M (actual acceleration of missile) goes infinity when the current time t closely approaches the total flight time t_f. In other words, the PNG system keeps stability in a finite time and it tends to unstable at the vicinity of the interception [19]. That type of system is called 'finite-

time stability' that is defined as when the system's trajectories are within a state-space region over a determined interval of time [20].

Using the previous alternative linearized PNG model, the simulation is completed for the analysis.

II.3.2. Simulation results

The Simulink model is made from the above alternative linearized PNG homing loop model. This is shown in Figure 12.
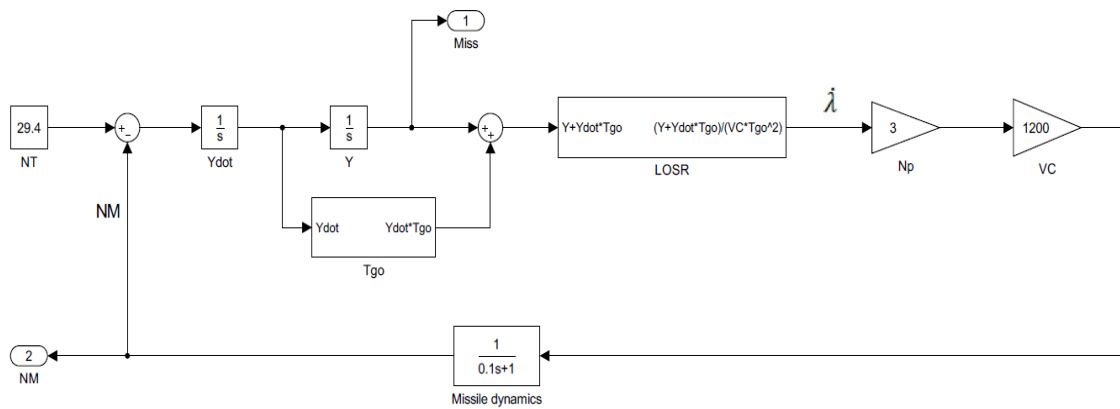
Figure 12. Linearized PNG homing loop model in Simulink

The parameter values of this Simulink model are same as those of the nonlinear model. This is for the comparison between the linearized model and the nonlinear model. For this, the information of the total flight of time t_F is acquired from the nonlinear model simulation results. For the study of the practical case, only the maneuvering target is simulated.

At first, a slow maneuvering target (3G) is simulated and the results are compared with the nonlinear model. The results are shown in Figure 13.
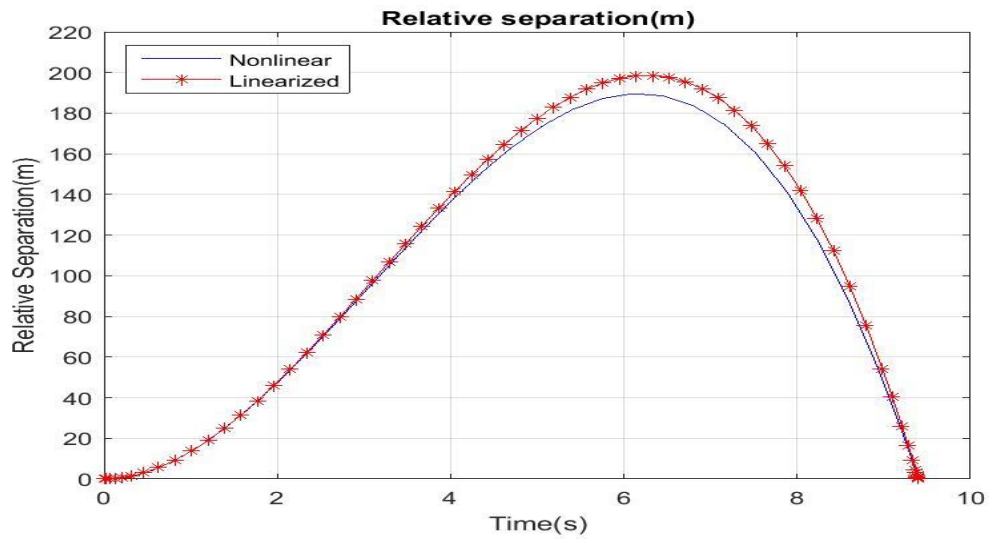
Figure 13.A. Relative separation comparison in case of 3G step in target maneuver($N' = 3$)
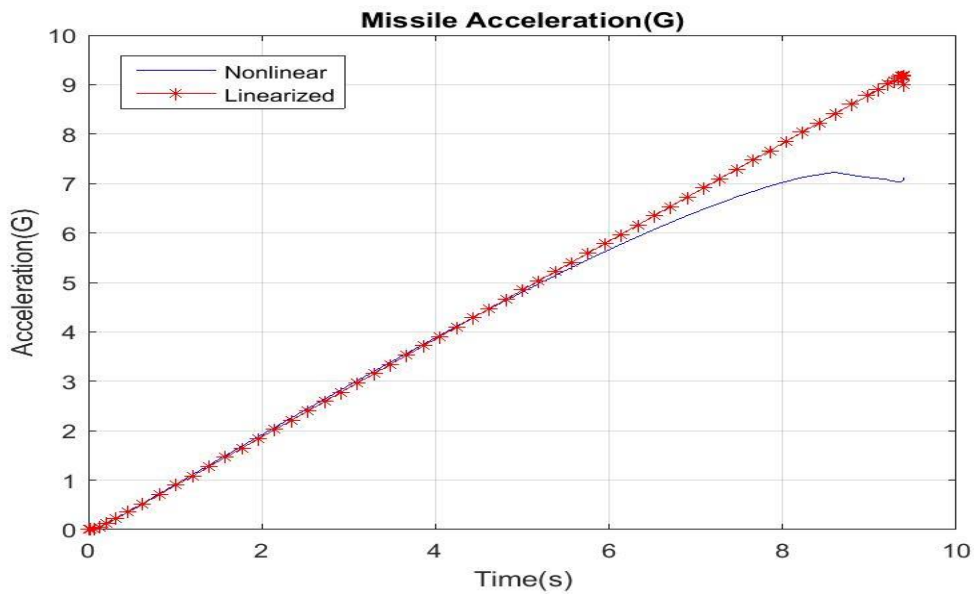
Figure 13.B. Missile acceleration comparison in case of 3G step in target maneuver($N^{'} = 3$)

From the Figure 13.A and B, it is observed that the linearized model overestimates the relative separation and the missile acceleration. The reason is that the linearized model assumes that the target y-axis acceleration magnitude is always the same throughout the engagement. But in the nonlinear model, the target y-axis acceleration magnitude decreases with a form of cosine function because the target is rotating. The reason for this estimation error about the target y-axis acceleration is explained in Figure 14.

Nonlinear PNG model estimation of target y-axis acceleration

Linearized PNG model estimation of target y-axis acceleration
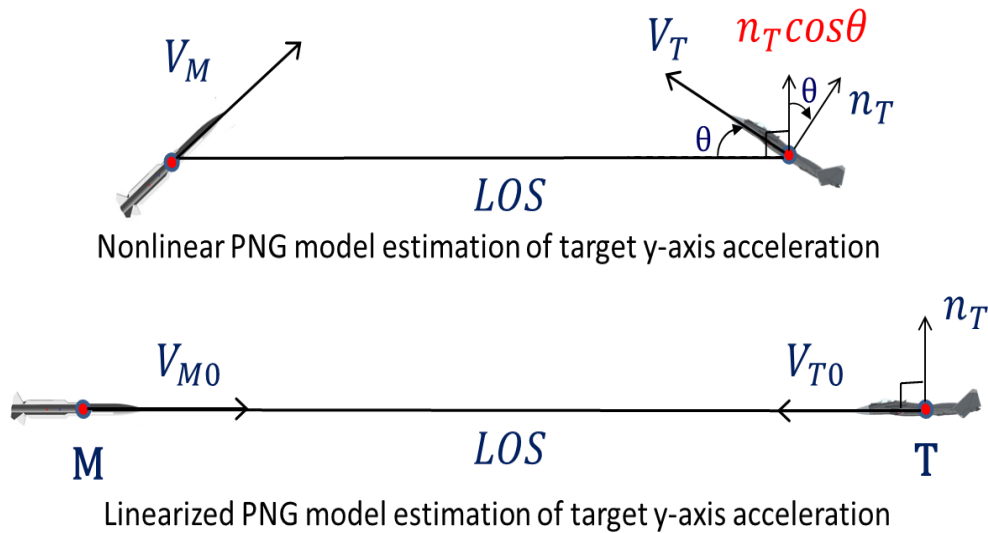
Figure 14. Reason of target y-axis acceleration estimation error

Hence, the required missile acceleration of the nonlinear model due to a target maneuvering is somewhat less than the linearized model, which is shown in Figure 13.B. Furthermore, this overestimated target y-axis acceleration of the linearized model leads to the discrepancy of the relative separation that is shown in Figure 13.A [13].

However, the important thing is the linearized model shows the trend of the missile acceleration profile, which monotonically increases for most of the flight time due to a target maneuver. Hence, we can conclude that the linearized model provides sufficient accurate estimation information about the relationship of parameters. Hence, the achieved information from the linearized model can be used in the controller design.

From the state-space representation of the linearized PNG model and the relative separation profile from the Figure 13.A, we can conclude the characteristics of the PNG. The missile acceleration of the PNG, 3rd state of the state-space model, goes to infinity (practically saturated) at the interception time, but the relative separation (y) goes to zero. Hence, the target interception can be achieved by the PNG.

To analyze the effect of the target maneuver increase on the LOSR, the slow maneuvering target(3G) and the fast maneuvering target(10G) are simulated. Figure 15 shows the LOSR profiles of the 2 cases. These profiles show the two characteristics of the PNG. First, the PNG cannot achieve its essential goal, which regulates the LOSR to zero to the maneuvering target. If the PNG works perfectly, the LOSR should converge and stay at zero until interception. But the linearized PNG model shows the linearly increasing LOSR in both cases. This result agrees with the LOSR profile of the nonlinear model which is shown in Figure 6.C.

Second, the LOSR increases as the target acceleration increases. This shows why the 2-D nonlinear PNG model fails to keep the collision triangle with the fast maneuvering target. Furthermore, the miss distance increases as the LOSR error increases.

36
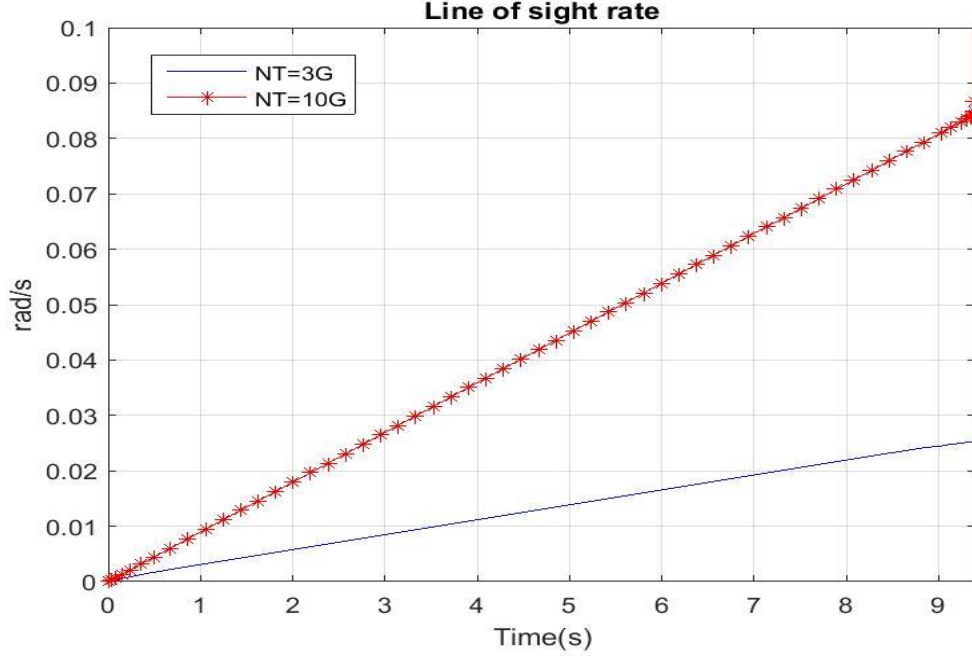
Figure 15. LOSR of the linearized PNG model with maneuvering targets(3G, 10G)

From this LOSR profile of the linearized PNG model, we can get a motive for using the servomechanism theory to solve this problem: Using an integral and take the LOSR to the input of the integral, it is possible to eliminate or minimize the LOSR. This idea becomes the motive of the PI guidance and the PID guidance.

To sum up, from the linearized PNG model, we can conclude the followings: (1) the PNG system maintains stability in the finite time and it becomes unstable at the interception time to the fast maneuvering target. (2) The PNG system shows the tendency that the LOSR increases as the target acceleration increases. Hence, it is possible to apply the servomechanism theory to minimize the LOSR error and, this may lead to the accurate missile system.

CHAPTER III

PID GUIDANCE

From the previous chapter, we saw that the conventional PNG is effective for the slow maneuvering target (3G) but has a limited performance for the fast maneuvering target (10G). Both of the nonlinear and the linearized models show the LOSR error to the maneuvering target and the LOSR increases as the target acceleration increases.

In this chapter, the theory of servomechanisms and its application to the missile guidance problem are studied. And the most widely used controller type in the servomechanism system, the PID controller is introduced in brief. Then, the PID guidance is introduced with its structure and characteristic.

III.1. Theory of servomechanisms

The central problems of control theory are (1) the tracking and (2) the disturbance rejection problem. The servomechanism problem is a tracking problem despite the inherent uncertainties and changes in the plant dynamics. The regulator problem, which is a special case of the servomechanism problem, makes the desired state to zero.

The secret of the servomechanism theory is based on an integrator. A simple integrator is shown in Figure 16.
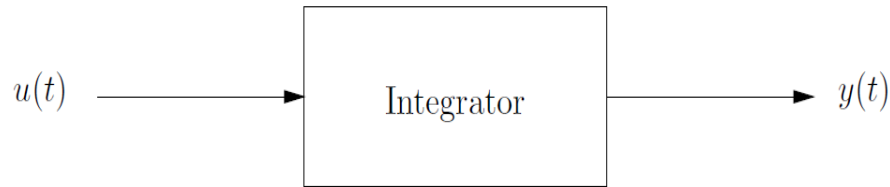
Figure 16. An integrator

The input-output equation is

$$y(t) = K \int_0^t u(\tau)d\tau + y(0) \qquad (47)$$

and this can be differentiated,

$$\frac{dy(t)}{dt} = Ku(t) \qquad (48)$$

where K is the integrator gain.

Now suppose that the plant is asymptotically stable, so the output y(t) is a constant. It follows from equation (48) that

$$\frac{dy(t)}{dt} = 0 = Ku(t) \text{ for all } t > 0. \qquad (49)$$

Equation (49) proves the operation of an integrator that if the output of an integrator is constant for a finite time, then the input must be zero in the same finite time [7].

This simple and powerful principle of an integrator is the basis of servomechanisms. This strength of the integrator can be applied to solve the PNG problem. From the viewpoint of the servomechanism theory, the PNG is simply a regulator problem which drives the LOSR to zero. If we use an integrator and make the LOSR the input of the integral, we can bring the LOSR to zero. Then, a guidance system without a miss distance can be achieved.

III.2.   Proportional-Integral-Derivative controller

The PID controller is the most widely used controller in the servomechanism system. The PID controller is based on an integrator and, the proportional controller and a derivative controller are added in parallel. The structure of the PID controller is shown in Figure 17.
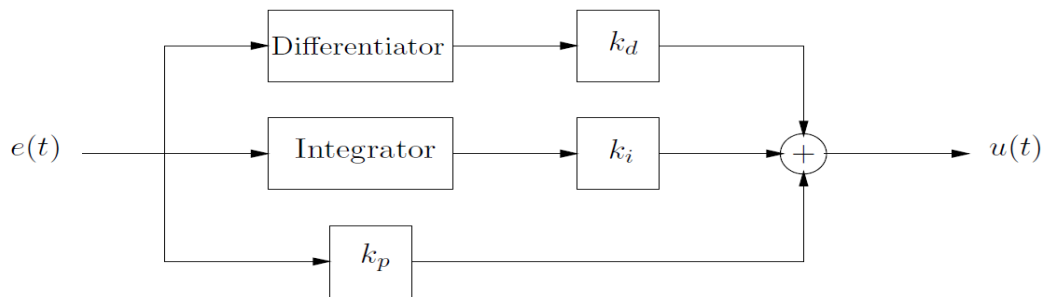
Figure 17. PID controller

The transfer function of the PID controller is,

$$C(s) = k_p + \frac{k_i}{s} + k_d s \qquad (50)$$

where k_p is the proportional term, k_i is the integral term, and k_d is the derivative term. Each term has its own function such as:

The proportional term causes a corrective control action proportional to the error itself.

The integral term gives a controller output that is proportional to the accumulated error. This has positive feature of ensuring the steady state error to zero with a step input. But the shortcoming of the integral is it has a pole at the origin so it can badly affect loop stability.

The derivative term gives a controller output which is proportional to the rate of change of the error. It is sometimes referred to as a predictive mode because of its dependence on the error trend. The shortcoming of the derivative action is its tendency to yield the large controller output in response to the high-frequency control errors, such as measurement noise [21].

The PID controller is based on the servomechanism theory. Hence, as long as the closed loop system is stable, the input of the PID controller is driven to zero independent of the gains. Thus, $k_p, k_i,$ and k_d can be freely used to stabilize the closed-loop system and to achieve the required performance criterion such as a good transient response and robustness of the system.

III.3.   PID guidance

To solve the performance limit of the conventional PNG model to the fast maneuvering target, the theory of servomechanism was applied to the missile guidance problem [10-12]. The goal of the missile guidance is regulating the LOSR to zero. Hence, the strength of an integrator fits to solve the PNG problem.

The structure of the PID guidance is shown in Figure 18. The difference of PID guidance from the PNG is the PID guidance replaces the effective navigation ratio N' with a PID controller. The other structures of PID controller are equal to the PNG.

Since the PID guidance is based on the structure of the PNG, the PID guidance shares the same characteristics of the PNG. (1)The PID guidance shows the finite time

stability. (2) The PID guidance shows that the LOSR increases as the target acceleration increases.

The strength of PID guidance is it can minimize the LOSR error with the integrator action. At the same time, the PID guidance can use the free gains for a good transient response and robust stability.

The design process of the PID guidance and the performance comparison between the two models will be studied in the next chapter.

$$MD = y(t_F)$$
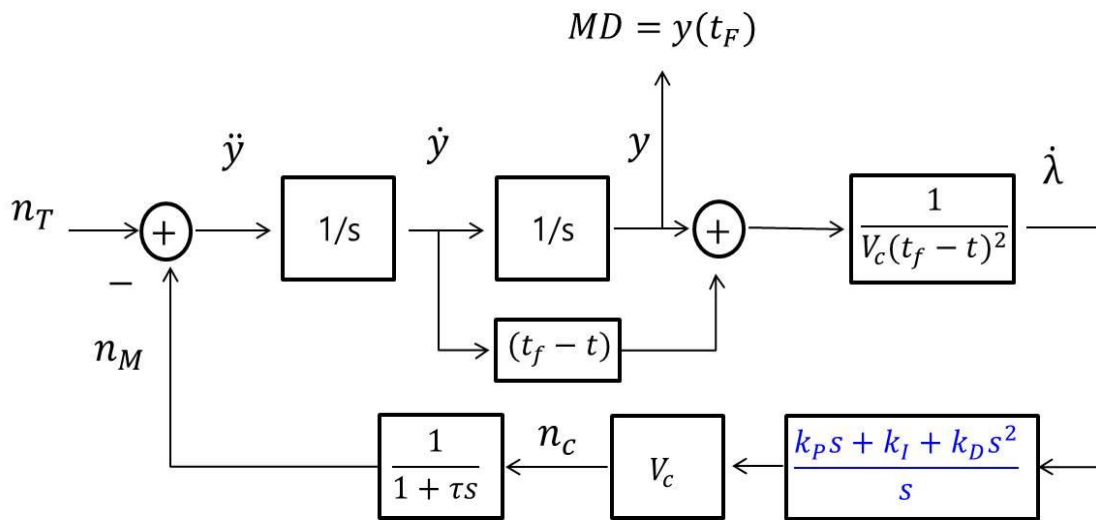
Figure 18. Linearized PID guidance homing loop

CHAPTER IV

PID GUIDANCE DESIGN

From the previous chapter, the concept of the servomechanism theory and the PID guidance are introduced. The key of the PID guidance is designing the set of PID controller for satisfying the performance criterion. In this chapter, the design process of PID guidance is studied and the performance of the designed guidance is compared with the conventional PNG model.

IV.1. PID guidance design by numerical method

In the conventional PNG, it is known that the effective navigation ratio(N') is chosen between 3 and 5 in practice considering the system noise effect. But in the PID guidance, the practical interval of the PID gains is not known clearly. Thus, in this study, the given interval of the PID gains is taken from the former references and it is shown in Table 6 [10, 12].

Table 6. Interval of PID gains for simulation

k_p	k_i	k_d
3 ~ 5	0 ~ 2	0 ~ 2

Based on the previous 2-D nonlinear missile and target engagement model, the PID guidance is simulated iteratively within the given interval of PID gains.

Since the defense missile should handle the various targets, this simulation was completed assuming the 2 scenarios: first scenario is for the aircraft target when the own missile velocity is faster than the aircraft target. Second scenario is for the missile target when the target velocity is faster than the own missile.

Simulation goal is finding the set of PID gains which satisfies the performance specification in both scenarios. The performance specification is chosen that the miss distance is less than 0.01 meter.

The designed PID guidance is compared with the conventional PNG model from the viewpoint of the miss distance accuracy and the capture region, since the missile should have the accuracy and wide capture region at the same time.

IV.1.1. Scenario 1: Aircraft target

The first scenario is intercepting the aircraft target. The target notices the interceptor missile at the start point of the terminal phase and does evasive maneuvers with the maximum acceleration consistently (10G). The initial condition of the first scenario is same as the previous fast maneuvering target in the Table 3.

Using the 2-D nonlinear engagement model iteratively, the simulation was completed within the given interval of gains. Each PID gain interval is evenly spaced with 5 points which is shown in Table 7. Thus, total 125 PID sets are simulated.

Table 7. Simulated PID gains

Gains	Spaced points
k_p	[3.0, 3.5, 4.0, 4.5, 5.0]
k_i	[0, 0.5, 1.0, 1.5, 2.0]
k_d	[0, 0.5, 1.0, 1.5, 2.0]

The PID sets satisfy the performance criterion (Miss distance < 0.01) are shown in Table 8. There are 53 sets that satisfy the performance criterion. From the given aircraft target scenario initial condition, we can choose one of the sets in the Table 8 which guarantees the performance criterion.

Table 8. Designed PID sets for scenario 1

k_p	k_i	k_d	Miss Distance(m)
3	2	1.5	0.000
3	2	2	0.000
3.5	2	0	0.002
3.5	2	0.5	0.000
3.5	2	1	0.000
3.5	2	1.5	0.000
3.5	2	2	0.000
4	0	2	0.000
4	1.5	1.5	0.000
4	1.5	2	0.000
4	2	0	0.002
4	2	0.5	0.000
4	2	1	0.000
4	2	1.5	0.000
4	2	2	0.000
4.5	0	1	0.000
4.5	0	1.5	0.000
4.5	0	2	0.000
4.5	0.5	2	0.000

Table 8. Continued

k_p	k_i	k_d	Miss Distance(m)
4.5	1	1.5	0.000
4.5	1	2	0.000
4.5	1.5	0	0.001
4.5	1.5	0.5	0.000
4.5	1.5	1	0.000
4.5	1.5	1.5	0.000
4.5	1.5	2	0.000
4.5	2	0	0.001
4.5	2	0.5	0.000
4.5	2	1	0.000
4.5	2	1.5	0.000
4.5	2	2	0.000
5	0	0.5	0.000
5	0	1	0.000
5	0	1.5	0.000
5	0	2	0.000
5	0.5	1	0.000
5	0.5	1.5	0.000
5	0.5	2	0.000
5	1	0	0.002
5	1	0.5	0.000
5	1	1	0.000
5	1	1.5	0.000
5	1	2	0.000
5	1.5	0	0.001
5	1.5	0.5	0.000
5	1.5	1	0.000
5	1.5	1.5	0.000
5	1.5	2	0.000
5	2	0	0.002
5	2	0.5	0.000
5	2	1	0.000
5	2	1.5	0.000
5	2	2	0.000

In Chapter II, the conventional PNG guidance showed the large miss distance (26.243 meters) when the effective navigation ratio N' was 5. Compared with the PNG model, we can see that the integral and derivative gains can yield the accurate miss distance.

Figure 19.A shows the trajectory comparison between the PNG and PID guidance. We can see that the PID guidance turns the missile slightly faster than the PNG. Otherwise, the trajectories are almost identical. The magnified picture of the trajectory is shown in Figure 19.B. We can see that the PID guidance steers the missile heading faster than the PNG at the end of engagement and accurately hits the target.

Figure 19.C shows the LOSR profile comparison between the PNG and the PID guidance. The PID guidance shows smaller LOSR and it remains stable for a longer period than the PNG model. Thus, this implies that the small and extended stability of LOSR leads to the miss distance accuracy.
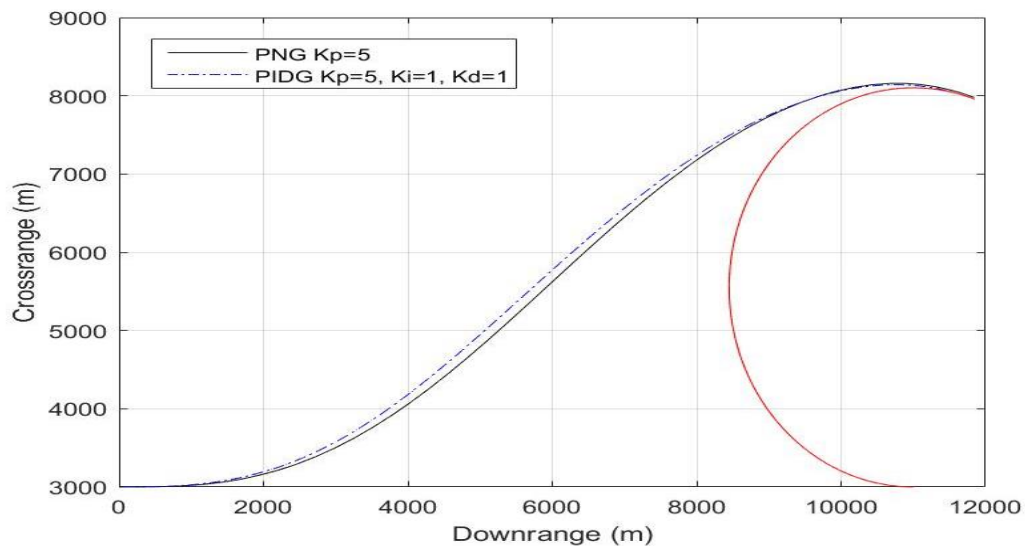

Figure 19.A. Trajectory comparison between PNG and PID guidance in scenario 1
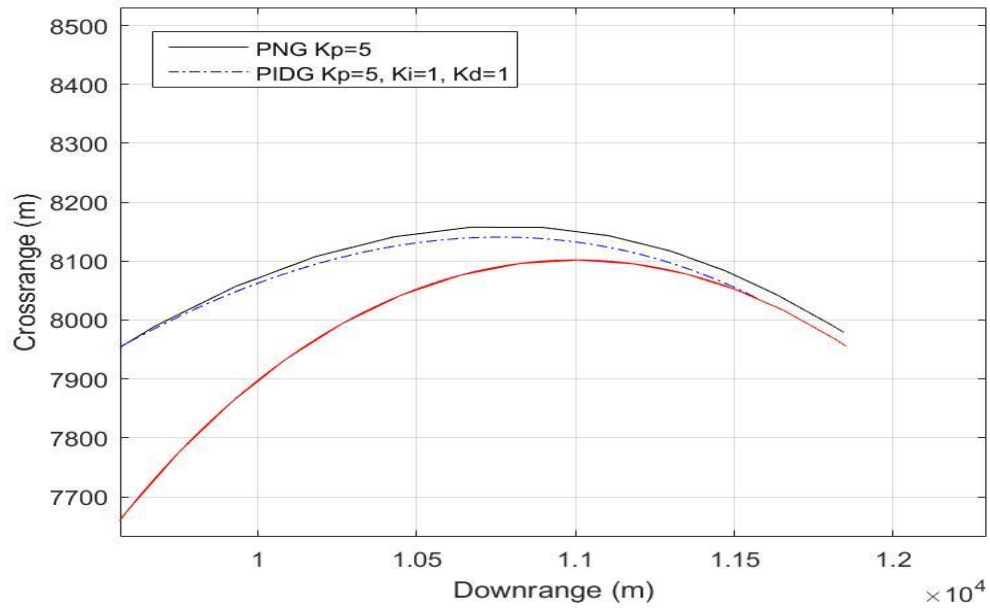
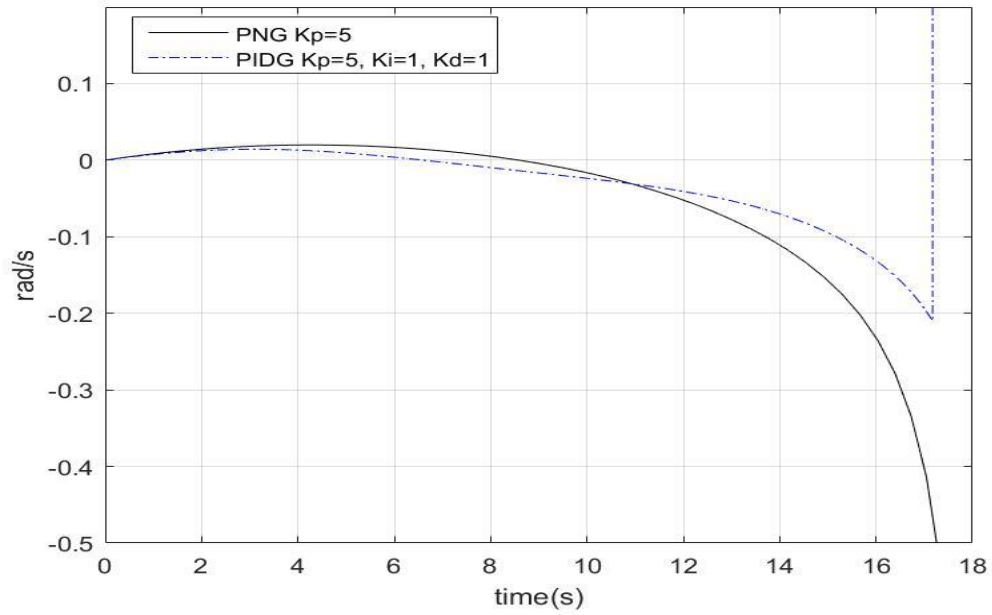Figure 19.B. Magnified trajectory of PNG and PID guidance in scenario 1

Figure 19.C. LOSR comparison between PNG and PID guidance in scenario 1

48

IV.1.2. Scenario 2: Missile target

In the air defense problem, not only the fighter aircraft but also the enemy missile is the primary threat. Thus, the designed missile guidance should have the capability to intercept the missile target which may have higher velocity and maneuverability. The initial condition of the scenario 2 is shown in Table 9.

Table 9. Initial condition of scenario 2

Missile		Target	
X-axis position(m)	0	X-axis position(m)	4,500
Y-axis position(m)	3,000	Y-axis position(m)	5,000
Velocity(m/s)	700	Velocity(m/s)	1,400
Flight velocity angle $\alpha(°)$	0	Flight velocity angle $\beta(°)$	0
Time constant(s)	0.1	Acceleration(G force)	-12
Maximum acceleration(G force)	20		

The simulation is completed within the same interval of PID gains. The PID sets are shown in Table 10 those satisfy the performance criterion in the scenario 2. It shows that there are only 24 sets for satisfying the performance criterion. Compared with the scenario 1, we can see that the higher set of PID gains is required to hit the fast maneuvering target.

Table 10. Designed PID sets for scenario 2

k_p	k_i	k_d	Miss distance(m)
4	2	1	0.000
4	2	1.5	0.000
4	2	2	0.000
4.5	1.5	1	0.000
4.5	1.5	1.5	0.000
4.5	1.5	2	0.000
4.5	2	0.5	0.000
4.5	2	1	0.000
4.5	2	1.5	0.000
4.5	2	2	0.000
5	1	0.5	0.000
5	1	1	0.000
5	1	1.5	0.000
5	1	2	0.000
5	1.5	0	0.000
5	1.5	0.5	0.000
5	1.5	1	0.000
5	1.5	1.5	0.000
5	1.5	2	0.000
5	2	0	0.004
5	2	0.5	0.000
5	2	1	0.000
5	2	1.5	0.000
5	2	2	0.000

Figure 20.A shows the trajectory comparison between the PNG and PID guidance. Like the scenario 1, the PID guidance steers the missile slightly faster than the PNG. The magnified trajectory from Figure 20.B shows the PID guidance makes the collision triangle and accurately intercepts the target.

Figure 20.C shows the LOSR comparison between the PNG and the PID guidance. Similarly with the scenario 1, the PID guidance shows smaller LOSR and longer stable time than the PNG and this is directly connected with the accurate miss distance of the PID guidance.
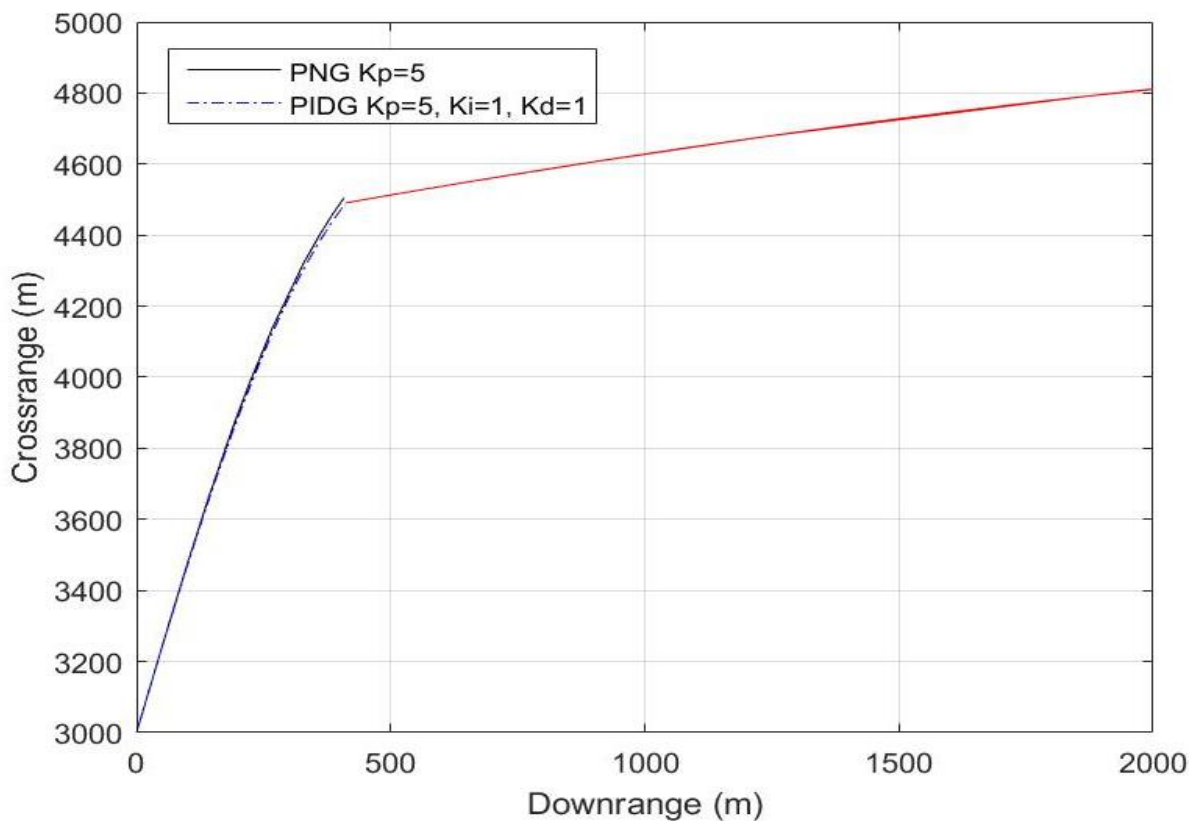

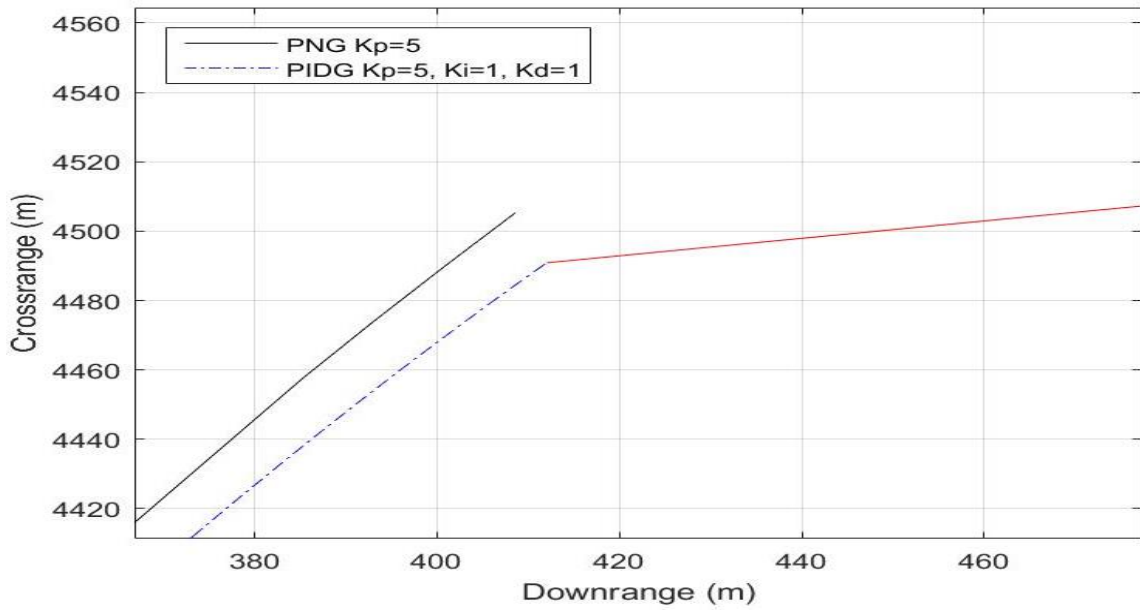Figure 20.A. Trajectory comparison between PNG and PID guidance in scenario 2

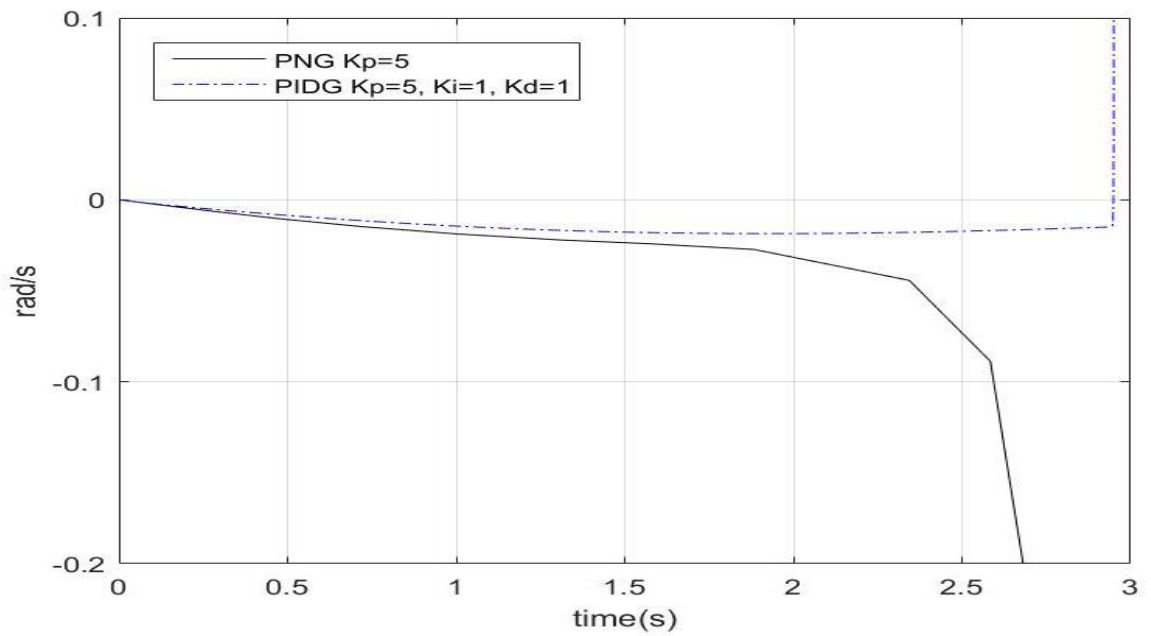Figure 20.B. Magnified trajectories of PNG and PID guidance in scenario 2

Figure 20.C. LOSR comparison between PNG and PID guidance in scenario 2

From the previous 2 simulations, the desired PID sets are achieved which can handle the both scenarios and those are summarized in Table 11. This shows that there are many options we can choose in the given interval of PID gains. To choose the appropriate PID set, the system characteristics should be considered. For example, if the missile guidance system is subject to system noise, the PI guidance should be used instead of the PID guidance. This consideration can narrow the appropriate PID sets [10].

Table 11. PID sets satisfying for scenario 1 and 2

PID guidance			Scenario 1	Scenario 1
k_p	k_i	k_d	Miss distance(m)	Miss distance(m)
4	2	1	0.000	0.000
4	2	1.5	0.000	0.000
4	2	2	0.000	0.000
4.5	1.5	1	0.000	0.000
4.5	1.5	1.5	0.000	0.000
4.5	1.5	2	0.000	0.000
4.5	2	0.5	0.000	0.000
4.5	2	1	0.000	0.000
4.5	2	1.5	0.000	0.000
4.5	2	2	0.000	0.000
5	1	0.5	0.000	0.000
5	1	1	0.000	0.000
5	1	1.5	0.000	0.000
5	1	2	0.000	0.000

PID guidance			Scenario 1	Scenario 1
k_p	k_i	k_d	Miss distance(m)	Miss distance(m)
5	1.5	0	0.001	0.000
5	1.5	0.5	0.000	0.000
5	1.5	1	0.000	0.000
5	1.5	1.5	0.000	0.000
5	1.5	2	0.000	0.000
5	2	0	0.004	0.004
5	2	0.5	0.000	0.000
5	2	1	0.000	0.000
5	2	1.5	0.000	0.000
5	2	2	0.000	0.000

IV.2. Capture region comparison

The initial relative position between missile and target can be varied depending on the each situation. Since the missile should handle the various relative positions, the capture regions are analyzed between the two models. The initial condition of this simulation is shown in Table 12.

Table 12. Initial condition for capture region comparison

Missile		Target	
X-axis position(m)	0	X-axis position(m)	0 ~ 5,000
Y-axis position(m)	0	Y-axis position(m)	0 ~ 5,000
Velocity(m/s)	700	Velocity(m/s)	500
Flight velocity angle α(°)	0	Flight velocity angle β(°)	0
Time constant(s)	0.1	Acceleration(G force)	10
Maximum acceleration(G force)	20		

To describe the various relative positions, the target x and y initial positions are evenly spaced with 250 meters which are shown in Table 13. Hence, each axis has 21 positions and total 441 sections showing the initial relative position are tested. Using the 2-D nonlinear engagement model iteratively, the simulation was completed.

Table 13. Initial positions of target

Axis	Position(m)
x	[0 250 500 750 1,000 1,250 ………. 4,000 4,250 4,500 4,750 5,000]
y	[0 250 500 750 1,000 1,250 ………. 4,000 4,250 4,500 4,750 5,000]

To evaluate the capturability of each relative position, new performance criterion is set based on the miss distance accuracy. Each section is colored based on the miss distance accuracy which is shown in Table 14. The section where the miss distance is greater than or equal to 10 meters is evaluated as the miss.

Table 14. Performance evaluation criterion for capture region

Miss Distance(MD) range(m)	Color
$MD < 0.01$	
$0.01 \leq MD < 0.1$	
$0.1 \leq MD < 1$	
$1 \leq MD < 10$	
$10 \leq MD$	

Figure 21.A and 21.B show the capture region of the PNG model and PID guidance model. The effective navigation ratio (N') of the PNG model is 5, and the parameter values of the PID guidance are $k_p = 5, k_i = 1$, and $k_d = 2$.
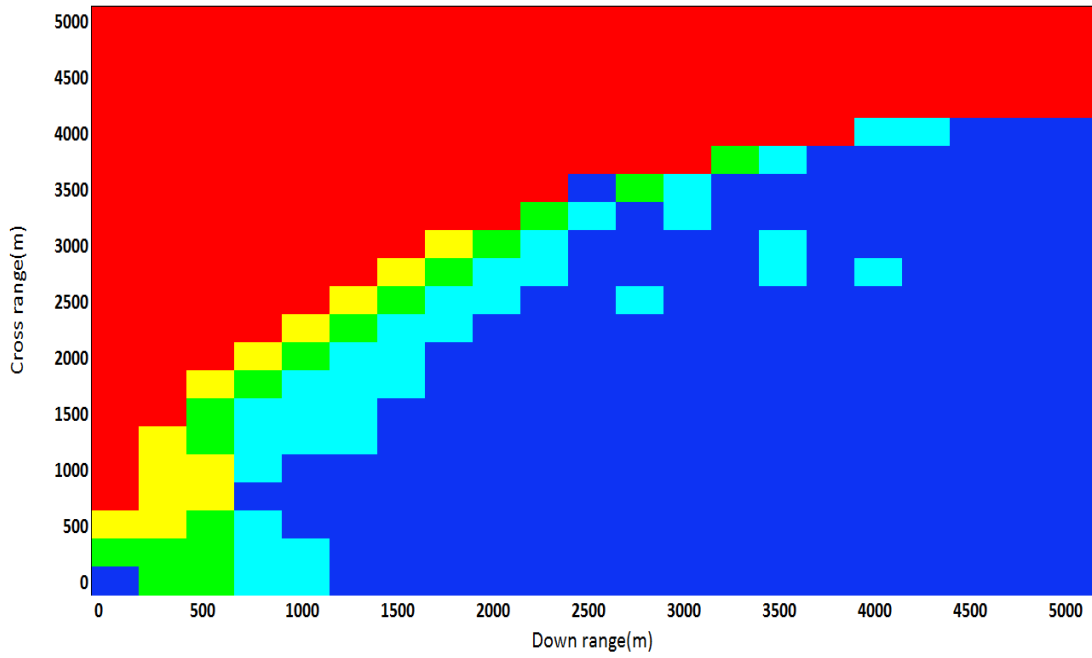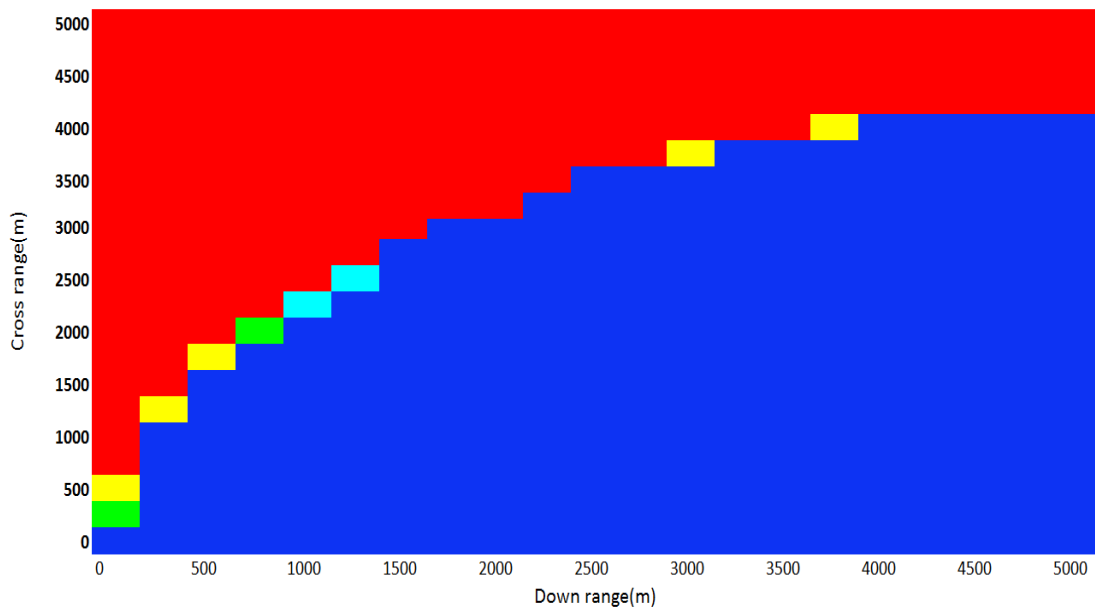
55

Figure 21.A. Capture region of PNG model ($N' = 5$)

Figure 21.B. Capture region of PID guidance model ($k_p = 5, k_i = 1, k_d = 2$)

The capture region comparison between the two models is shown in Table 15.

Table 15. Capture region comparison between PNG and PID guidance

Miss Distance(MD) range (m)	Color	PNG (ea)	PID guidance (ea)	Variation (ea)
MD < 0.01		213	270	+57
0.01 ≤ MD < 0.1		34	2	-32
0.1 ≤ MD < 1		17	2	-15
1 ≤ MD < 10		13	5	-8
10 ≤ MD		164	162	-2
Total		441	441	0

The PID guidance increases 57 blue-colored sections compared with the PNG. This shows that the PID guidance yields an improved accuracy in 57 sections where the PNG is less accurate or misses the target. Furthermore, the PID guidance decreases 2 red-colored (miss) sections than the PNG. This shows that the PID guidance increases the 2 capturable sections. Hence, we can see that the PID guidance can improve the miss distance accuracy and the capture region.

At the same time, this simulation implies that the missile performance improvement by the controller design alone is limited if the velocity of the missile is fixed. Figure 22 shows the capture region of the PID guidance when the missile speed is increased from 700m/s to 1,000m/s. The parameter values of PID guidance are same with the previous simulation ($k_p = 5, k_i = 1, k_d = 2$). We can see that the faster missile

speed can increase the capture region considerably. In other words, the controller design and the missile speed should be improved together to get a wider capture region.
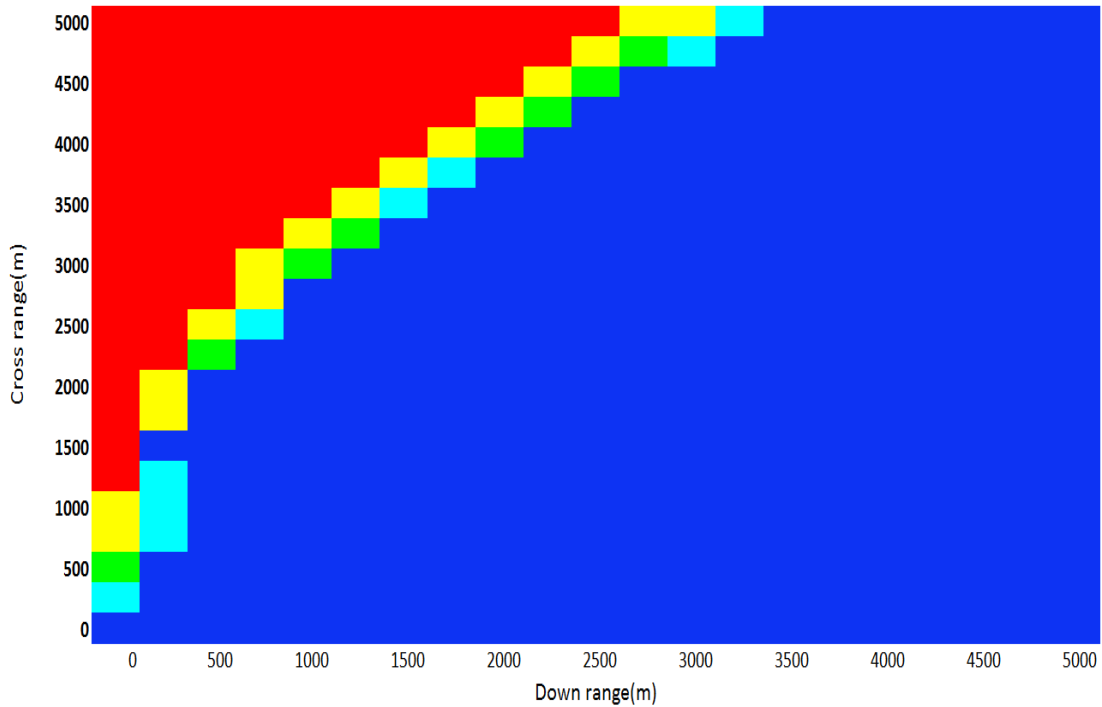
Figure 22. Capture region of PID guidance model when $V_M = 1,000m/s$

To sum up, the design process of PID guidance is studied considering the various target scenarios. The designed PID guidance shows the effectiveness in the miss distance accuracy and capture region. At the same time, the PID guidance reveals its limit that the expansion of capture region is limited by controller design alone.

In the next chapter, the designed PID guidance is tested in the three-dimensional (3-D) model to validate its effectiveness.

CHAPTER V

THREE-DIMENSIONAL MODEL APPLICATION

From the previous chapter, the designed PID guidance shows better performance than the PNG in the 2-D nonlinear engagement model. In this chapter, the PID guidance model is expanded to the three-dimensional (3-D) model. The 3-D model is called the Three Plane Approach (TPA) and this model is taken from Moran and Altilar[22].

V.1. Introduction

The TPA model is based on the mathematical equations of the previous 2-D nonlinear engagement model. In the TPA, the 3-D engagement space is projected onto three perpendicular planes: S_{xy}, S_{xz}, and S_{yz}. For example, the projections of the missile velocity vector on to those planes are shown in Figure 23.
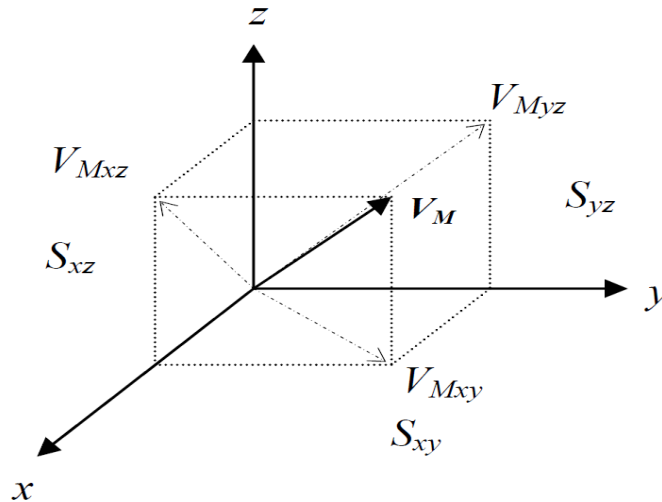
Figure 23. Projection of missile velocity vector onto 3 planes, reprinted from [22]

Likewise, the target velocity is projected on those planes. The projected target and missile velocities and their relative motion geometry are shown in Figure 24.

The approach of TPA is solving the guidance problem in the 3-D space by projecting onto 3 perpendicular planes. Then solve the guidance problem in each plane independently using the 2-D PNG model and combing these 2-D solutions to produce the 3-D solution.

A. S_{xy} Plane

B. S_{XZ} Plane

C. S_{yz} Plane

Figure 24. The projections of missile's and target's relative motion onto 3 planes, reprinted from [22]

V.2. Mathematical model
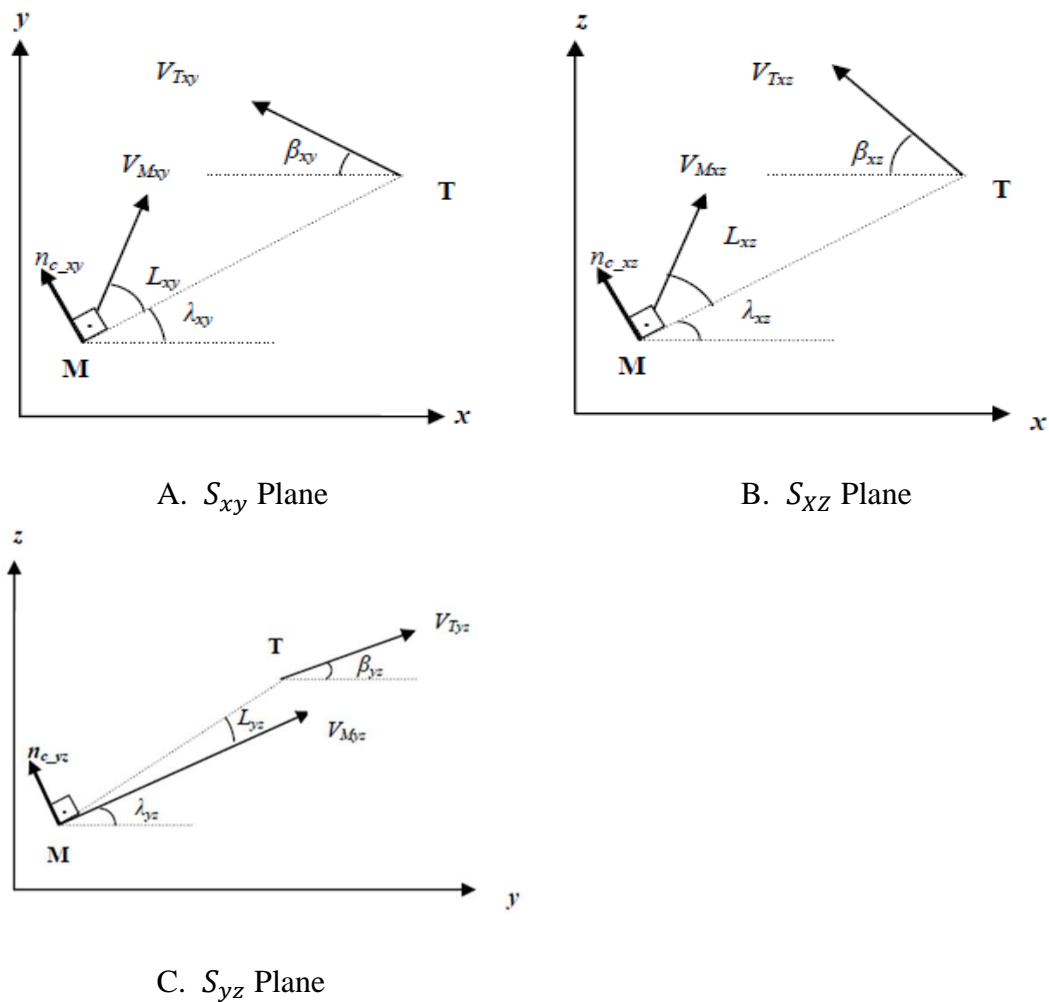
From the Figure 23 and 24, the procedures of solving each plane's guidance problem and combining to the 3-D model are followed:

The range between the missile and the target is:

$$R_{TM} = \sqrt{R_{TMX}^2 + R_{TMY}^2 + R_{TMZ}^2} \tag{51}$$

The LOS angles are:

$$\lambda_{XY} = \tan^{-1}(\frac{R_{TMY}}{R_{TMX}}) \tag{52}$$

$$\lambda_{XZ} = \tan^{-1}(\frac{R_{TMZ}}{R_{TMX}}) \tag{53}$$

$$\lambda_{YZ} = \tan^{-1}(\frac{R_{TMZ}}{R_{TMY}}) \tag{54}$$

Target flight-path angles are:

$$\beta_{XY} = \tan^{-1}(\frac{V_{TY}}{V_{TX}}) \tag{55}$$

$$\beta_{XZ} = \tan^{-1}(\frac{V_{TZ}}{V_{TX}}) \tag{56}$$

$$\beta_{YZ} = \tan^{-1}(\frac{V_{TZ}}{V_{TY}}) \tag{57}$$

Target velocity vector projections onto S_{xy}, S_{xz}, and S_{yz} planes are:

$$V_{TXY} = \sqrt{V_{TX}^2 + V_{TY}^2} \tag{58}$$

$$V_{TXZ} = \sqrt{V_{TX}^2 + V_{TZ}^2} \tag{59}$$

$$V_{TYZ} = \sqrt{V_{TY}^2 + V_{TZ}^2} \tag{60}$$

Missile lead angles L_{XY}, L_{XZ}, and L_{YZ} for each plane are:

$$L_{XY} = \sin^{-1}(\frac{V_{TXY} \cdot \sin(\beta_{XY} + \lambda_{XY})}{V_M}) \tag{61}$$

$$L_{XZ} = \sin^{-1}\left(\frac{V_{TXZ}\cdot\sin(\beta_{XZ}+\lambda_{XZ})}{V_M}\right) \qquad (62)$$

$$L_{YZ} = \sin^{-1}\left(\frac{V_{TYZ}\cdot\sin(\beta_{YZ}+\lambda_{YZ})}{V_M}\right) \qquad (63)$$

It is shown from the PNG formula that to produce the missile acceleration command for each plane, their closing velocity and the rate of change of the line-of-sight angle (LOSR) must be calculated. The LOSR projections onto each plane are:

$$\dot{\lambda}_{XY} = \frac{R_{TMX}V_{TMY}-V_{TMX}R_{TMY}}{R_{TMX}^2+R_{TMY}^2} \qquad (64)$$

$$\dot{\lambda}_{XZ} = \frac{R_{TMX}V_{TMZ}-V_{TMX}R_{TMZ}}{R_{TMX}^2+R_{TMZ}^2} \qquad (65)$$

$$\dot{\lambda}_{YZ} = \frac{R_{TMY}V_{TMZ}-V_{TMY}R_{TMZ}}{R_{TMY}^2+R_{TMZ}^2} \qquad (66)$$

The closing velocities on each plane can be defined as the negative rate of change of the range between the missile and the target. Therefore,

$$V_{CXY} = -\dot{R}_{TMXY} = -\frac{(R_{TMX}V_{TMX}+R_{TMY}V_{TMY})}{\sqrt{R_{TMX}^2+R_{TMY}^2}} \qquad (67)$$

$$V_{CXZ} = -\dot{R}_{TMXZ} = -\frac{(R_{TMX}V_{TMX}+R_{TMZ}V_{TMZ})}{\sqrt{R_{TMX}^2+R_{TMZ}^2}} \qquad (68)$$

$$V_{CYZ} = -\dot{R}_{TMYZ} = -\frac{(R_{TMY}V_{TMY}+R_{TMZ}V_{TMZ})}{\sqrt{R_{TMY}^2+R_{TMZ}^2}} \qquad (69)$$

where the relative velocities on each plane are:

$$V_{TMX} = V_{TX} - V_{MX} \qquad (70)$$

$$V_{TMY} = V_{TY} - V_{MY} \qquad (71)$$

$$V_{TMZ} = V_{TZ} - V_{MZ} \qquad (72)$$

Hence, the commanded missile accelerations onto each plane from the PNG are:

$$n_{CXY} = N'V_{CXY}\dot{\lambda}_{XY} \tag{73}$$

$$n_{CXZ} = N'V_{CXZ}\dot{\lambda}_{XZ} \tag{74}$$

$$n_{CYZ} = N'V_{CYZ}\dot{\lambda}_{YZ} \tag{75}$$

Missile acceleration components for x, y, and z-axis are generated by combining two acceleration commands sharing the same axis. Figure 24 implies that one axis' acceleration component interacts with the two planes' acceleration commands. Using the trigonometric function, the unified missile acceleration components of axes x, y, and z can be calculated as:

$$\dot{V}_{MX} = -n_{CXY}\sin(\lambda_{XY}) - n_{CXZ}\sin(\lambda_{XZ}) \tag{76}$$

$$\dot{V}_{MY} = n_{CXY}\cos(\lambda_{XY}) - n_{CYZ}\sin(\lambda_{YZ}) \tag{77}$$

$$\dot{V}_{MZ} = n_{CXZ}\cos(\lambda_{XZ}) + n_{CYZ}\sin(\lambda_{YZ}) \tag{78}$$

Using the differential equations listed above a 3-D nonlinear missile and target engagement model with the PNG is made with MATLAB/Simulink.

Furthermore, to build the 3-D PID guidance model, the effective navigation ratio(N') in each plane is replaced with the PID controllers. The top level Simulink model is showed in Figure 25. Initial conditions and specifications of the missile and the target for this simulation are given in Table 16. The performance criterion for this simulation is chosen that the miss distance is less than 0.01 meter.
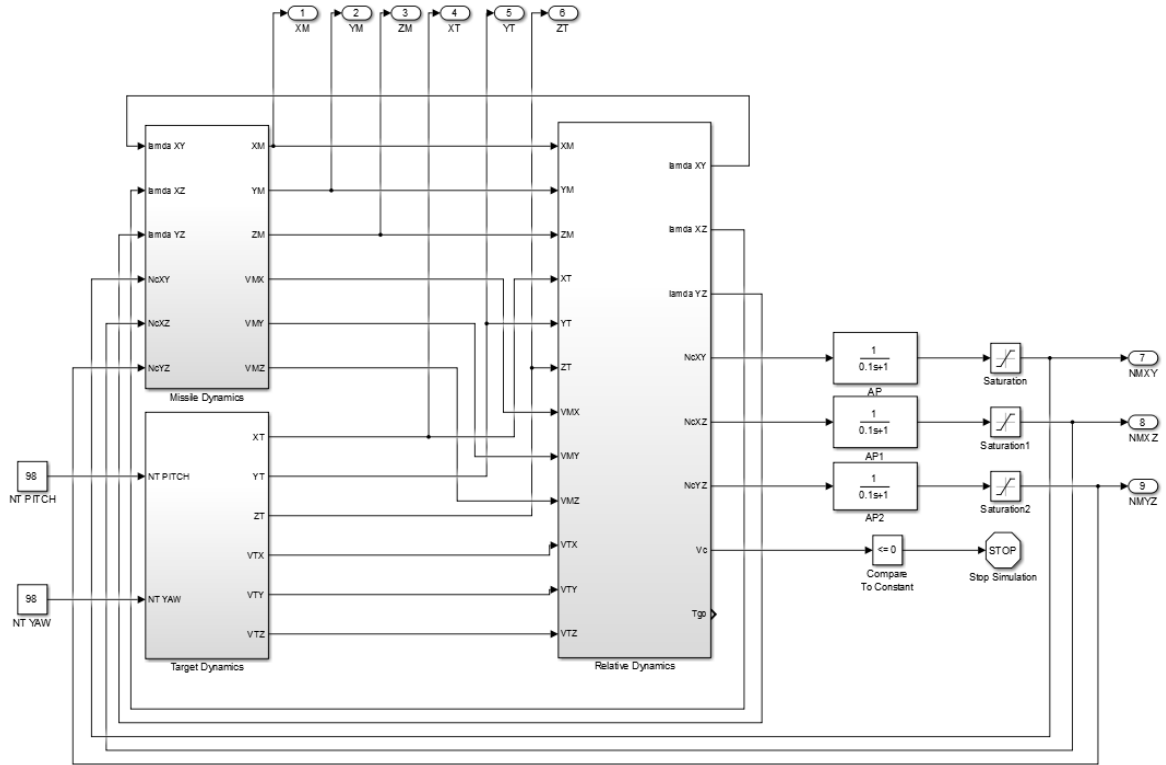
Figure 25. 3-D nonlinear engagement model in Simulink

Table 16. Initial condition of the 3-D nonlinear engagement model

Missile		Target	
X-axis position(m)	0	X-axis position(m)	3,000
Y-axis position(m)	0	Y-axis position(m)	3,000
Z-axis position(m)	3,000	Z-axis position(m)	3,000
Velocity(m/s)	900	Velocity(m/s)	500
Pitch angle(°)	0	Pitch angle(°)	0
Yaw angle(°)	0	Yaw angle(°)	0
Time constant(s)	0.1	Pitch acceleration(G force)	8
Maximum acceleration(G force)	20	Yaw acceleration(G force)	8

V.3. Simulation results

Under the initial condition of Table 15, the PNG and the PID guidance models are simulated and the results are compared. The effective navigation ratio (N') of the PNG model is 5, and the parameter set of the PID guidance is chosen form the designed sets in Table 11 as $k_p = 5, k_i = 1.5,$ and $k_d = 0.5$.

The two models' 3-D trajectories are compared in Figure 26.A. It shows that those two guidance laws' trajectories are almost identical. The performance difference between the two guidance laws is clearly shown in Figure 26.B. We can see that the PID guidance decreases the miss distance and satisfies the performance criterion. The simulation results between the two guidance laws are shown in Table 17.
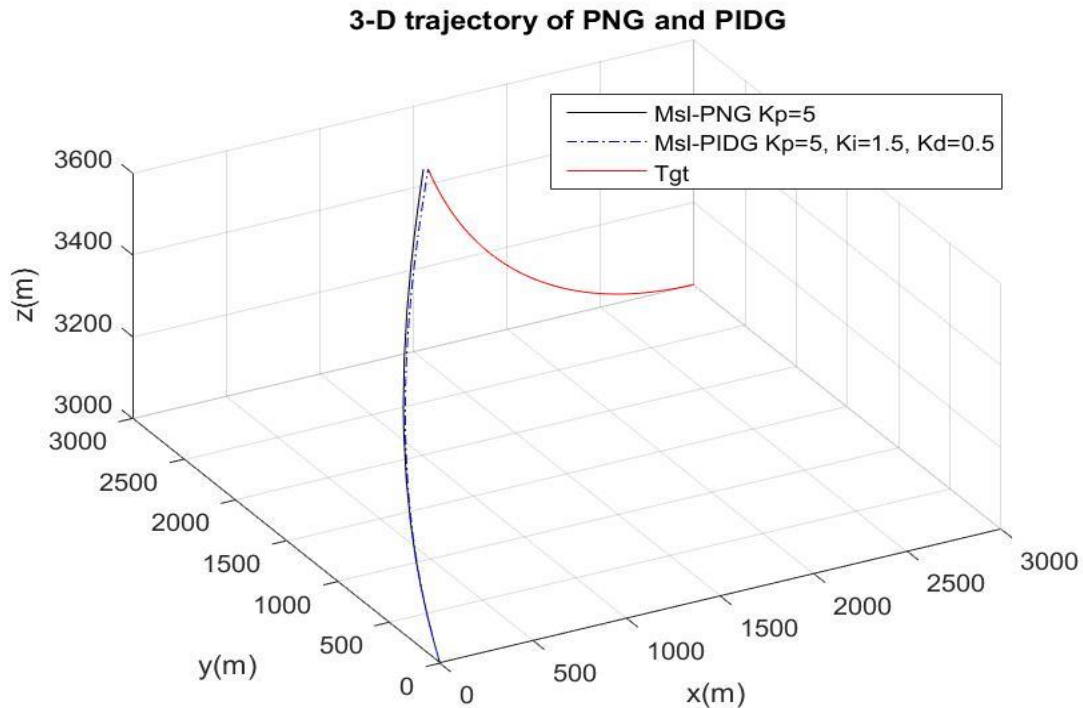

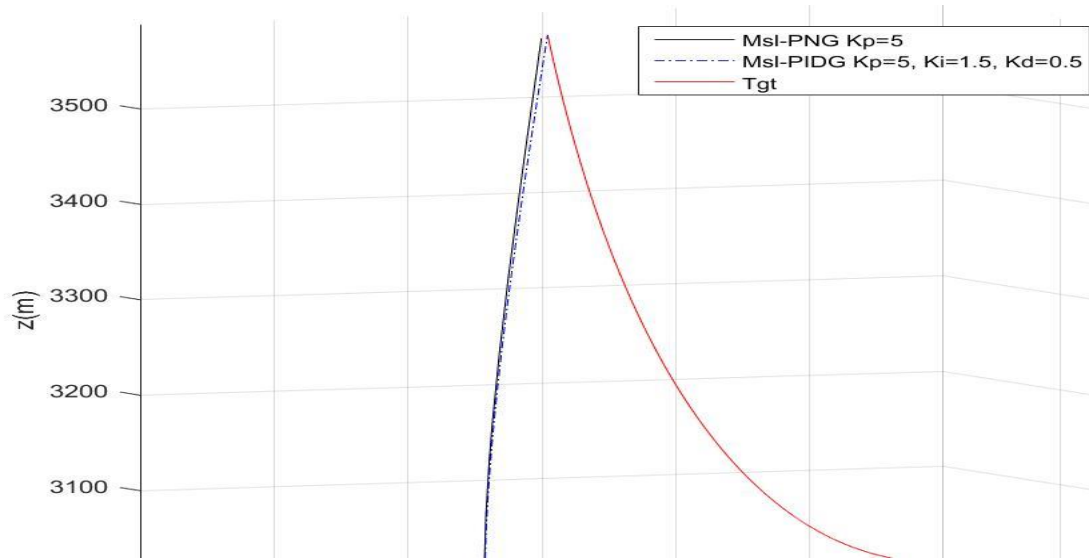Figure 26.A. 3-D trajectories comparison between PNG and PID guidance

Figure 26.B. Magnified 3-D trajectories of PNG and PID guidance

Table 17. 3-D simulation results between PNG and PID guidance

Guidance Laws	Intercept time(s)	Miss distance(m)
PNG	3.884	26.413
PID guidance	3.898	0.000

The projected trajectories on each plane are shown in Figure 27. The trajectories onto xy and yz plane clearly show that the PID guidance works effectively to the fast maneuvering target in the 3-D model.
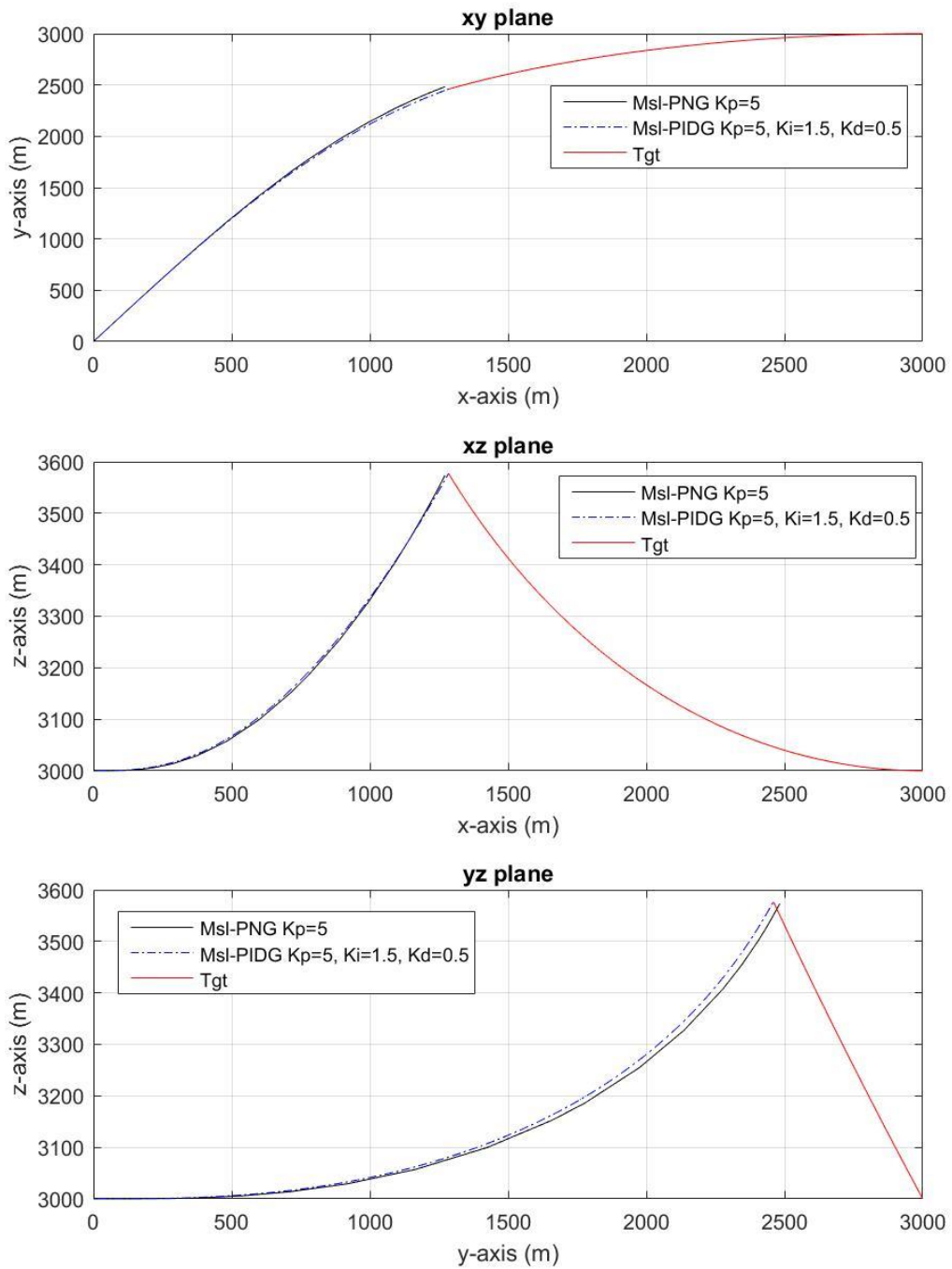
Figure 27. Trajectory projection on each plane

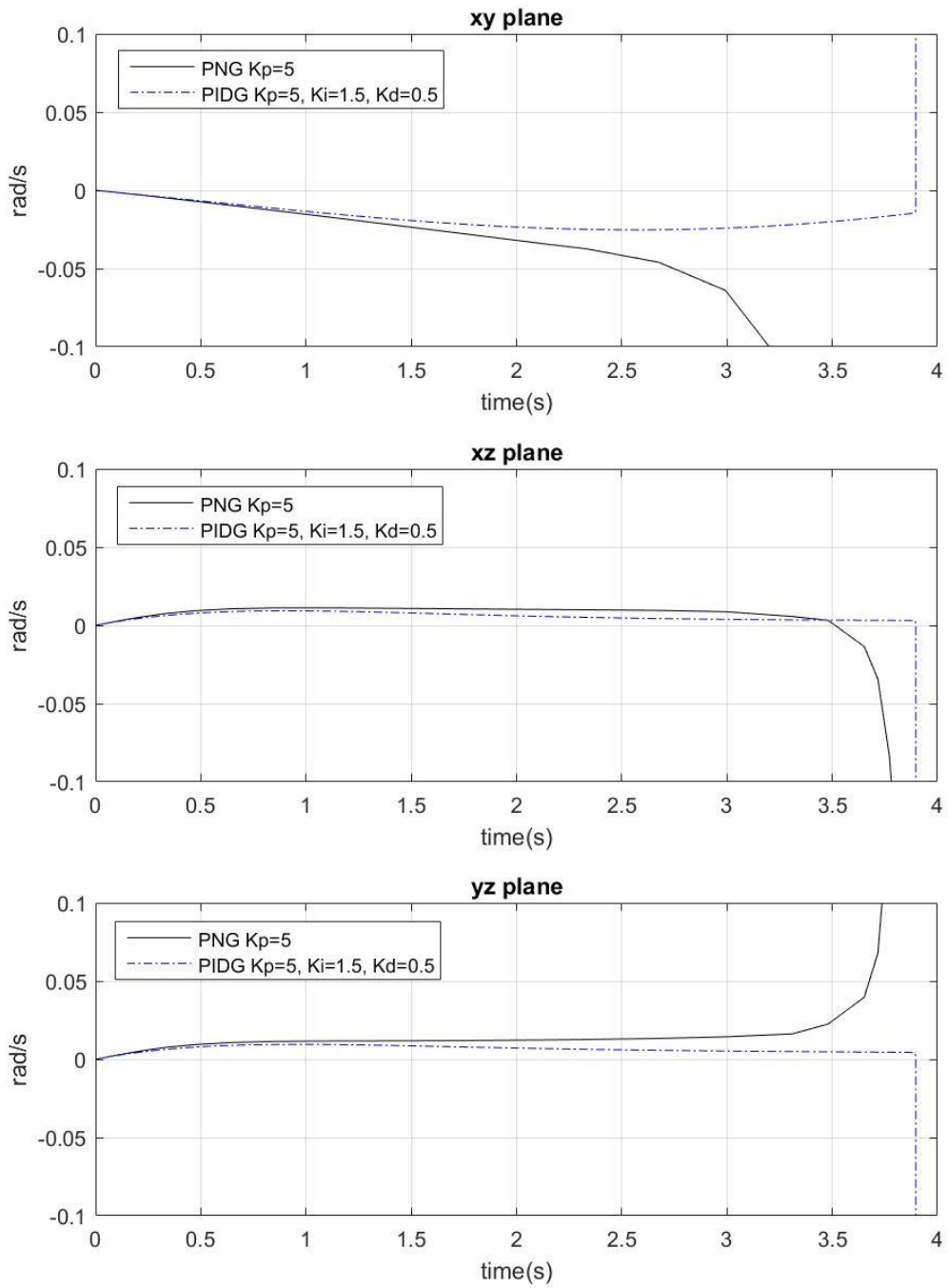The projected LOSR profiles on each plane are shown in Figure 28.

Figure 28. Projected LOSR on each plane

It is shown that the PID guidance shows smaller LOSR and extended stable time than the PNG. We can see that this result agrees with the previous 2-D nonlinear engagement model result.

To sum up, we identified that the PID guidance shows improved miss distance accuracy in the 3-D model. The reason is the PID guidance can minimize the LOSR and extend the finite stable time. This shows that the extended stability of missile guidance system directly leads the accurate performance.

From this result, the PID guidance scheme validates its effectiveness in the 3-D model.

CHAPTER VI

SUMMARY

In this thesis, the missile guidance problem using the PID controller is studied. The designed PID guidance shows miss distance accuracy against the fast maneuvering target. It is shown that this effectiveness is given from the decreased LOSR error and extended finite stable time. Furthermore, the PID guidance shows wider capture region, at the same time, it reveals its performance limit. Finally, the designed PID guidance validates its effectiveness in the 3-D model. The PID guidance is a possible solution to enhance the miss distance accuracy and capture region in existing homing missiles based on the PNG scheme with maintaining their current simple structures.

REFERENCES

[1]   N. F. Palumbo, R. A. Blauwkamp, and J. M. Lloyd, "Modern homing missile guidance theory and techniques," *Johns Hopkins APL Tech. Dig*, vol. 29, no. 1, pp. 42-59, 2010.

[2]   C. Dictionary. (2002, Jun. 1). Cambridge dictionaries online [Online]. Available: http://dictionary.cambridge.org/us/dictionary/english/missile. Accessed Jun. 1, 2016.

[3]   G. M. Siouris, *Missile guidance and control systems*, New York, NY: Springer Science & Business Media, 2004.

[4]   US Navy. (2016). Fact File - Standard Missile [Online]. Available: http://www.navy.mil/navydata/fact_display.asp?cid=2200&tid=1200&ct=2. Accessed Jun.1, 2016.

[5]   E. Berglund, "Guidance and Control Technology," presented at the RTO SCI Lecture series on "Technologies for Future Precision Strike Missile Systems", Stockholm, Sweden, 2001.

[6]   C.-F. Lin, *Modern navigation, guidance, and control processing*, Englewood Cliffs, NJ: Prentice Hall, 1991.

[7]   S. P. Bhattacharyya, A. Datta, and L. H. Keel, *Linear control theory: structure, robustness, and optimization*, Boca Raton, FL: CRC press, 2009.

[8]   U. S. Shukla and P. R. Mahapatra, "The proportional navigation dilemma-pure or true?," *IEEE Trans. Aerosp. and Electron. Syst.,* vol. 26, pp. 382-392, Mar. 1990.

[9]   P. G. Gonsalves and A. K. Caglayan, "Fuzzy logic PID controller for missile terminal guidance," in *Intelligent Control, 1995., Proceedings of the 1995 IEEE International Symposium on*, Monterey, CA, 1995, pp. 377-382.

[10]   C.-M. Lin, C.-F. Hsu, S.-K. Chang, and R.-J. Wai, "Guidance law evaluation for missile guidance systems," *Asian J. of Control,* vol. 2, pp. 243-250, 2000.

[11]   R. Steve, "Missile Guidance Comparison," in *AIAA Guidance, Navigation, and Control Conference and Exhibit*, Providence, Rhode Island, 2004, pp. 1-4.

[12]   M. Golestani and I. Mohammadzaman, "PID guidance law design using short time stability approach," *Aerosp. Sci. and Technol.,* vol. 43, pp. 71-76, Jun. 2015.

[13]   P. Zarchan and American Institute of Aeronautics and Astronautics., *Tactical and strategic missile guidance*, 6th ed. Reston, VA: American Institute of Aeronautics and Astronautics Publications, 2012.

[14]   D. Bucco and R. Gorecki, "On Alternative Formulations for Linearised Miss Distance Analysis," Defence Sci. and Technol. Org., Edinburgh, Australia, Tech. Rep. DSTO-TR-2845, May 2013.

[15]   D. Sadler, "The mathematics of collision avoidance at sea," *J. of Navigation,* vol. 10, pp. 306-319, Oct. 1957.

[16]   J. Morrel, "The physics of collision at sea," *J. of Navigation,* vol. 14, pp. 163-184, Apr. 1961.

[17]   H. Cho, C.-K. Ryoo, A. Tsourdos, and B. White, "Optimal Impact Angle Control Guidance Law Based on Linearization About Collision Triangle," *J. of Guidance, Control, and Dynamics,* vol. 37, pp. 958-964, May 2014.

[18]   M. Webster. (2006, Jan.). Merriam-Webster online dictionary [Online]. Available: http://www.merriam-webster.com/dictionary/relative%20velocity. Accessed Jun. 1, 2016.

[19]   P. Gurfil, M. Jodorkovsky, and M. Guelman, "Finite Time Stability Approach to Proportional Navigation Systems Analysis," *J. of Guidance, Control, and Dynamics,* vol. 21, pp. 853-861, Nov. 1998.

[20]   S. Pradeep and S. Shrivastava, "Stability of dynamical systems-An overview," *J. of Guidance, Control, and Dynamics,* vol. 13, pp. 385-393, May 1990.

[21]   G. C. Goodwin, S. F. Graebe, and M. E. Salgado, *Control system design,* Upper Saddle River, NJ: Prentice Hall, 2001.

[22]   I. Moran and D. T. Altilar, "Three Plane Approach for 3D True Proportional Navigation," in *AIAA Guidance, Navigation, and Control Conference*, San Francisco, CA, 2005, pp. 3-10.